sustainability

MDPI

Article

Morphometric Evaluation and Its Incidence in the Mass Movements Present in the Chicamocha Canyon, Colombia

Joaquín Andrés Valencia Ortiz * and Antonio Miguel Martínez-Graña

Department of Geology, Faculty of Sciences, University of Salamanca, Plaza de los Caídos s/n, 37008 Salamanca, Spain
* Correspondence: andresval166@usal.es

Abstract: The dynamic behavior of the basins evaluated by their morphometric parameters establishes a relationship with the endogenous and exogenous factors of the earth that control the modeling of the rocky massif by weathering and erosion processes. The characterization of these relationships can define the degree of affectation of the surfaces and the agents that control them as a categorical element in the definition of scenarios within the planning of physical and natural territory. This evaluation considers parameters contained within the characterization of the relief, shape and texture of the drainage and the mobility of the flow in the basin. As a result of this evaluation, three factors were obtained that control the processes in the basins: a tectonic structural factor followed by climate control and, finally, seismic activity that plays an important role in the mechanical weathering of surfaces. The correlation of these factors showed that the Umpalá, Guaca, Río Negro, Cantabara and La Cureña basins display a high degree of physical and mechanical weathering of the rocky massif and that the Manco, Talarcuta, Las Pavas, Felisco and El Abra basins are more likely to generate torrential flows. The joint evaluation of these parameters provides a useful tool to understand the dynamic behavior of basins and their impact on anthropogenic setting.

Keywords: basins; morphometry; weathering–erosion; rock massif; Bucaramanga fault; torrential flows

check for updates

Citation: Valencia Ortiz, J.A.; Martínez-Graña, A.M. Morphometric Evaluation and Its Incidence in the Mass Movements Present in the Chicamocha Canyon, Colombia. *Sustainability* **2023**, *15*, 1140. https://doi.org/10.3390/su15021140

Academic Editor: Lóránt Dénes Dávid

Received: 21 December 2022
Revised: 3 January 2023
Accepted: 4 January 2023
Published: 7 January 2023

Copyright: © 2023 by the authors. Licensee MDPI, Basel, Switzerland. This article is an open access article distributed under the terms and conditions of the Creative Commons Attribution (CC BY) license (https://creativecommons.org/licenses/by/4.0/).

1. Introduction

In recent decades, hydrometeorological conditions have generated a considerable increase in the manifestations of processes of instability on surfaces (mass movements). These conditions are possibly being caused by a significant climate change that is represented by an increase in average, maximum and minimum air temperatures that provide rainfall scenarios with greater intensity and recurrence, especially in mountainous areas where they can easily trigger mass movement events due to major changes in the ground surface [1–5].

At the global level, the effects generated by mass movements have caused drastic damage to infrastructure of different kinds, as well as victims and human losses. A study conducted by the World Health Organization between 1998 and 2017 showed that mass movements affected 4.8 million people and caused more than 18,000 deaths [6,7]. In addition to the above, there is a substantial increase in the manifestations of events related to climate activity, especially rainfall, as well as anthropogenic elements that are affected by seismic activity [8]. These events have generated considerable loss of human life and infrastructure, with an estimated damage reported by Swiss Re for 2011 of USD 370 billion in losses of anthropogenic elements and the natural environment [9]. Within these climatic conditions, floods are one of the most influential factors worldwide, since, according to a study that examined the period between 1985 and 2009, floods represent 40% of all natural disasters [10].

In a more regional context, climatic conditions have triggered events such as floods and mass movements that have affected the infrastructure and generated loss of human life with incidents reported for the years 1998, 2010, 2011, 2013 and 2020 by the Inventory System of

Disasters—DesInventar [11]. Within the context of characterization of an environment that is disturbed by climatic and/or internal conditions of the earth, it is necessary to estimate the degree of affectation that may occur on anthropic and natural environments [12,13]. To establish these degrees of affectation, it is necessary to start from models defined by parametric and non-parametric functions on a fundamental unit in a regional analysis, and which in this case are based on the study of the hydrographic basin. This is because the basin describes this dynamic behavior in the same system containing patterns and/or behaviors typical of the surrounding atmosphere. Conditions such as floods, which occur with greater recurrence, together with the degradation of the rock massif, which may be susceptible to mass movements, respond to events of the torrential flows, landslides and falls that affect these environments. One of the conditions within the analysis of hydrographic basins is their morphometric characterization, which can include several factors that define the modeling of their surfaces.

Factors such as tectonic and structural condition and climatic behavior are closely related to the control of the shape, size, slope, texture of the surfaces of the hydrographic basins, as well as condition the processes of weathering and erosion of these surfaces [14,15]. The morphometric analysis from a quantitative perspective determines the properties or punctual, linear, area and volumetric parameters of the relief [16,17]. This evaluation allows to explain the geological and geomorphological history of each river basin from the quantitative perspective providing a description of the physiography and/or the behavior of the drainage system [18–20]. The evaluation of the basin employs defined parameters for the characterization of the drainage system, the analysis of the mobility of the flow, the texture of the channel and characterization of the relief. The included parameters are the Size of the basin (A), Basin length (Lb), ratio of the Drainage bifurcation (Rb), Form factor (Rf), Drainage density (Dd), Drainage texture (T), Torrential coefficient (Ct), Basin concentration time (Tc), Asymmetry factor (Af), Hypsometric curve, Compactness coefficient (Kc), Massive coefficient (Cm), Orographic coefficient (Co), Sinuosity of mountain front (Smf), Ruggedness number (Rn), Stream length–gradient Index (SL) and Reason for valley width and valley altitude (Vf) [16,21–25].

With the evaluation of each one of these parameters added to the analysis of the factors that condition the dynamic control of each hydrographic basin, studies focused on the dynamic behavior of surfaces and flows can be carried out. This type of analysis serves as a useful tool when evaluating the functioning of the hydrological system of a region and thus contributing to the management of natural resources [26–28], which, in turn, provides a basis for integration into territorial policies, complying with current regulations on issues related to territorial planning and disaster risk management, and providing an input from the quantitative and qualitative description of the basins, hydrographic for their morphometric parameters.

Under this approach, the present study focuses on an evaluation of surface dynamics that create unstable conditions on the slopes (mass movements) and qualitatively determines the ways in which these processes can affect anthropogenic elements. It is clear that the dynamics of the basins in relation to slope instability events are closely related to the degradation of the rock massif and the concentration of rainfall in each hydrographic basin. Therefore, complementary to the research approach, these morphometric parameters that are related to tectonic, structural, climatic, and seismic activity elements are quantified as precursors of weathering and erosion processes that trigger mass movement of different types such as, landslides, flow, and fall.

2. Regional Setting

The study area is located north of Bogotá, Colombia in a sector within the Chicamocha Canyon region, Santander. The total study area extends over 1357.62 km^2 and is subdivided by 16 hydrographic basins (Figure 1).

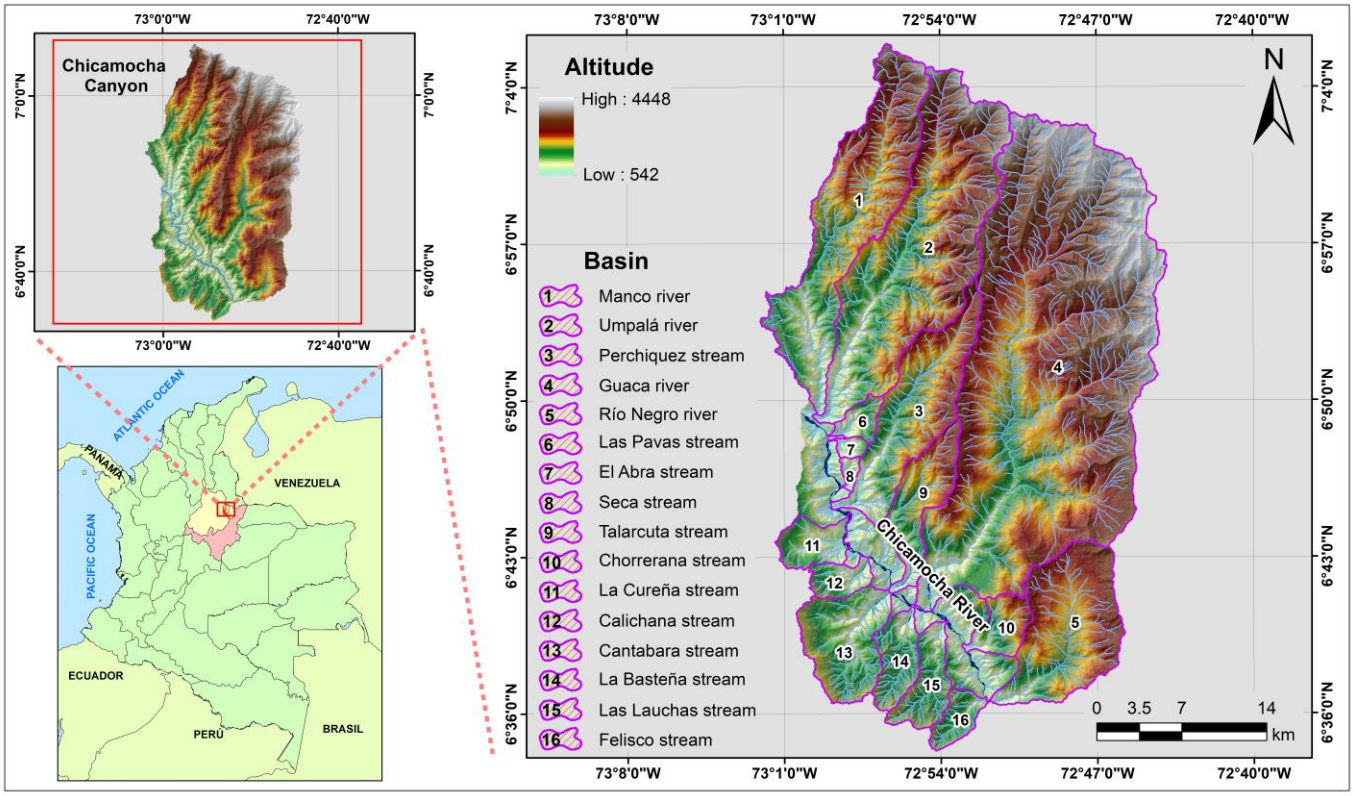

Figure 1. Location of the study area with delimitation of the hydrographic basins.

The study area has an altitude of between 542 m to 4448 m with an average of 1743 m, with a slope of between 0° to 78°, an average of 28.24° and a domain in the range of between 22° and 27°, with surfaces that are mostly oriented to the west (247.5° to 292.5°) (Figure 2). The drainage pattern is defined as being mainly subparallel, parallel to subdendritic. The region is characterized by having a climate strongly controlled by the topography and the Intertropical Convergence Zone (ITCZ), where temperature and rainfall (annual average values) can range from 8° to 16° C and 2000 mm to 2500 mm in the upper regions of the basins, up to 20–26° and 400–900 mm in the lower parts, respectively [29]. The correlation of precipitation data with evapotranspiration values (500 to 1600 mm/year) [30], according to the Holdridge classification, and areas of dry to very dry tropical xerophytic sub-desert forests are described, characterized by cacti and shrubs with very small leaves to avoid evapotranspiration; they are located in the lower parts of the basins. In the high mountain areas (upper part), there are areas of humid forests [31].

These climatic conditions generate important and rooted changes in the surfaces (lower region of the basins), leading to the creation of canyons and slopes of moderate to high slope associated with dry and warm climates; on the other hand, in the upper parts, there are wetter areas associated with topographic expressions of plateaus that develop on the Santandereano Massif [32]. Due to these climatic and topographic contrasts, the surfaces of these regions develop superficial, shallow, skeletal, and very eroded soils, where there is a predominance of rhosolic entisol-type soils [33]. In addition, Rangel-Ch and Cadena [33] assert that depending on the topographic aspect, two large groups of soils can be differentiated: (1) Present on slopes with gentle to steep slopes, with poorly evolved soils, low content of organic matter, rate of erosion equal to or greater than soil formation and where leaching processes are frequent. (2) At the edges of tributaries in sites with soils of medium content of organic matter, poor in soluble phosphorus and where the main agricultural work of the region has been developed.

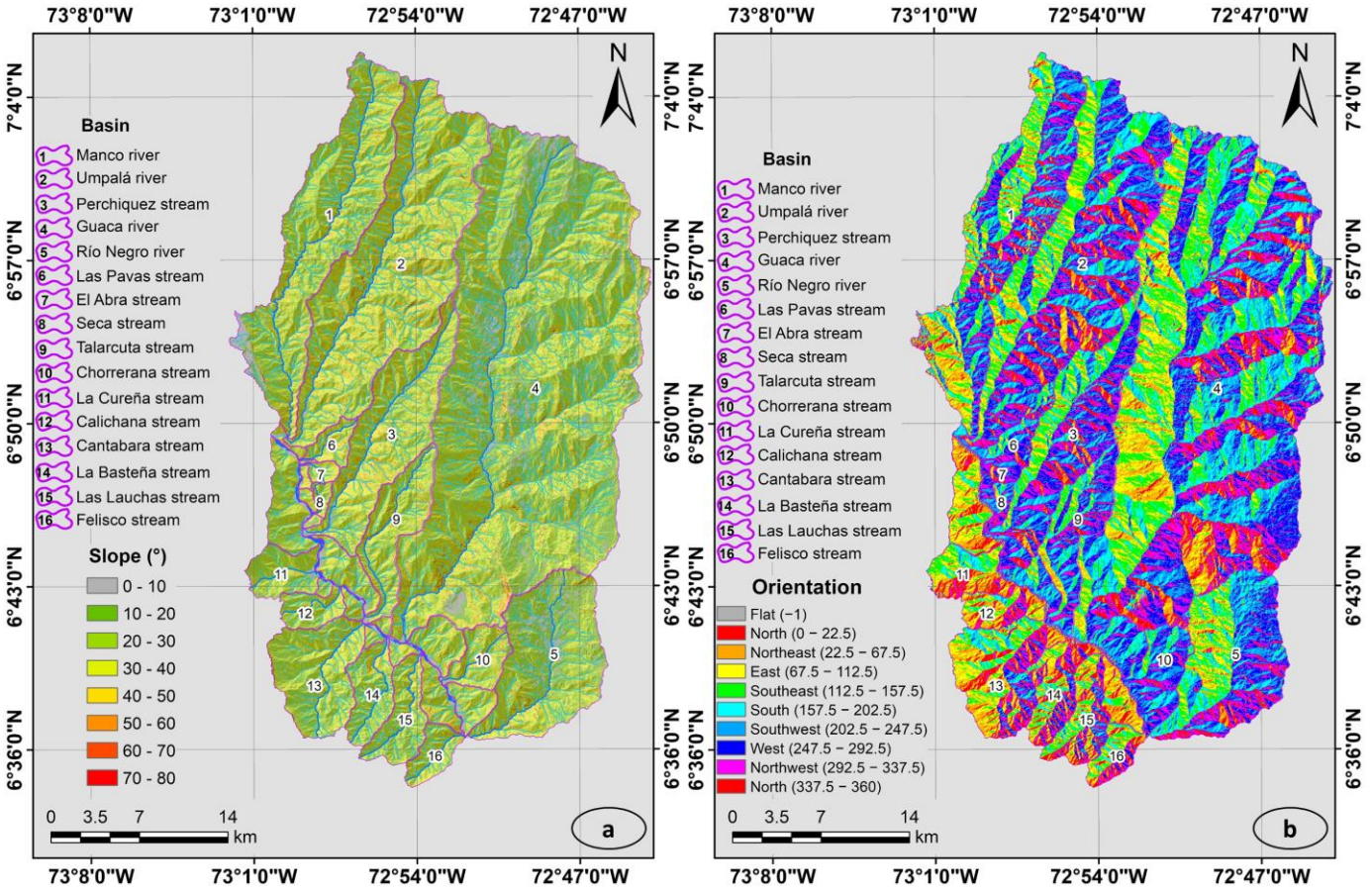

Figure 2. (**a**) Map of slopes. (**b**) Orientation map.

3. Geological and Geomorphological Context

In the study region, rocks from the Precambrian to the Quaternary period (Holocene epoch) are present (Figure 3). The rocks of Precambrian (PD) present schists, gneiss and migmatites. For the Pre-Devonian and Devonian period (D), phyllites, schists, and quartzites are generated, as well as siltstones and yellowish-gray shale. For the Triassic period(TR), sandstones and shales are presented; in the Jurassic period(J), pink granite and alaskites, pink biotitic quartzmonzonite, white biotitic quartzmonzonite, siltstone, fine-grained sandstone, conglomeratic sandstone, and conglomerates are generated [34–36].

In the Cretaceous period (K), rocks are generated with different compositions such as clear quartz sandstones, with intercalations of gray to brown siltstones, white to gray sandstones; intercalations of black shale, locally sandy; black clays, dark gray limestones; quartzite white sandstones, quartzite white sandstones; laminated black clays, fossiliferous limestones; dark gray shale; clay limestone and chert; greenish grey shale, limonitic nodules [35–37]. In the Quaternary period, materials are deposited that are the product of the processes of erosion and weathering of the surrounding massifs; they are distinguished by their transport mechanism that can be of fluvial or hydrogravitational type. Among these deposits are terraces and cones of dejection (Qal) with a lithology of rounded to subrounded clasts, of size between coarse sands to pebble, in a clayey sand matrix, as well as deposits of fluvial transport of size between fine sand to gravel, rounded to subrounded; colluvial, slopes, and collapse (Qc), with rock fragments of size between pebble and boulder, angular to subangular [34–37].

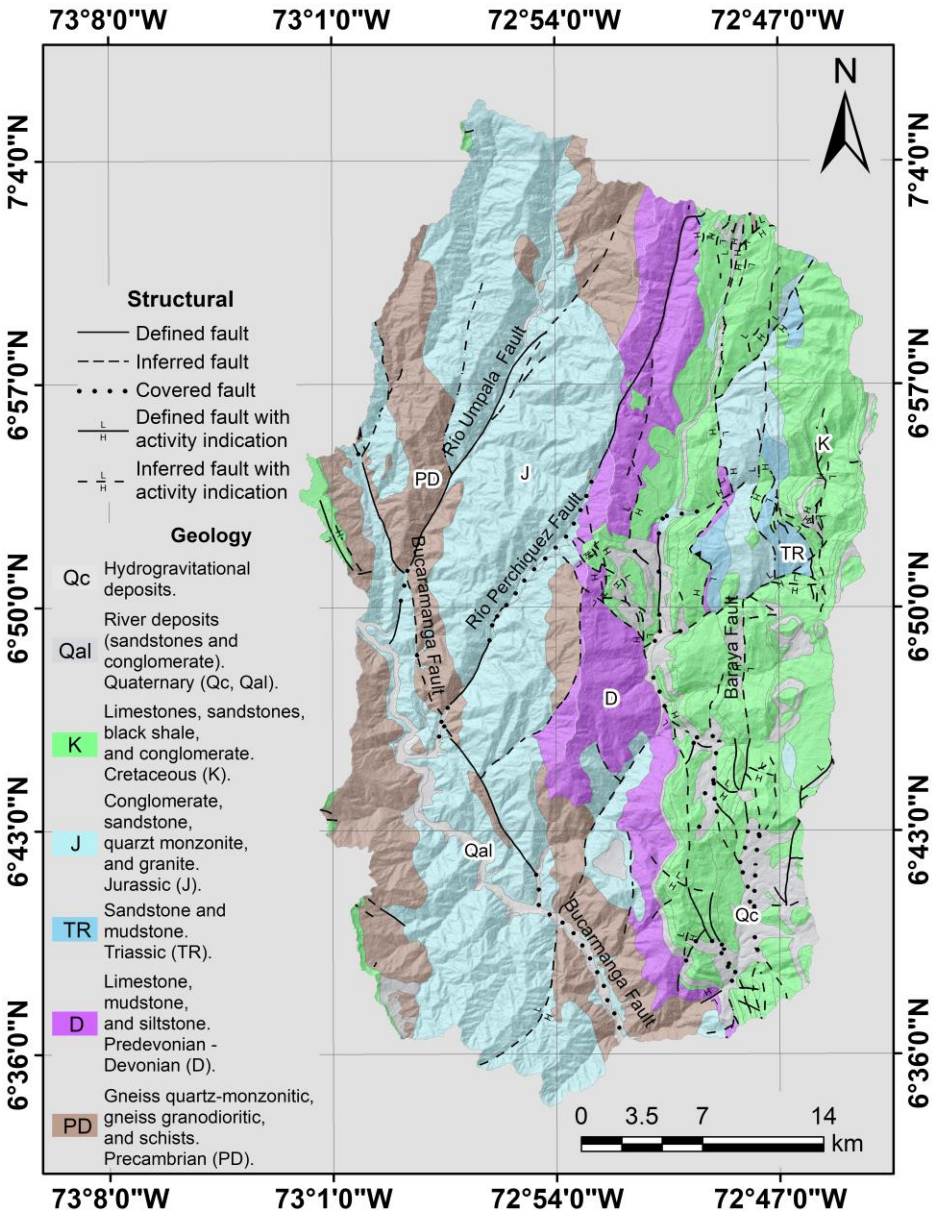

Figure 3. Geological map of the study area. Modified from the geological map at scale 1:100,000, Colombian Geological Service, sheet 109, 110, 120, 135, and 136 [34–38].

The structural arrangement of the region is framed mainly by the layout of the Bucaramanga Fault which is a regional type structure with a combined component in the course (sinistral) and in the dip (reverse) patterns [39,40]. On the other hand, there are Manco River Faults, Umpalá River and Perchiquez River, with a northeast direction that extends from the Bucaramanga fault, on igneous and metamorphic rocks. These faults, when they cut the Bucaramanga fault, produce right lateral displacements [36]. Baraya Fault presents a northerly direction; with a low-angle dip (locally), it contactspre-Cretaceous rocks with Cretaceous. Finally, there is Morro de las Peñas Fault that presents similar kinematics to Baraya Fault, but the latter is a little further north than the previous one [36].

For the region, a geomorphological control of a structural type is presented where structurally controlled loin units, flexural hooks and controlled basins are developed. These units, such as the loin, generate large block slide as a back-tilting on the left surface of Chicamocha River in response to the decompensation of the balance profile of the slope, causing its staggered appearance [41]. In addition, by the interaction of the faults present, fragile deformations are generated on the rocks surrounding the trace of the faults, which

give rise to multiple fractures of a systematic and penetrative nature that originate a centimeter of tabular cataclastic foliation. With this relationship added to the climatic conditions, a large amount of particulate material develops, giving rise to deposits of types of dejection cones, alluvial fans, and terraces [41].

4. Materials and Methods

To address the morphometric characterization of the hydrographic basins from a quantitative analysis, the elements defined within the physiographic characteristics of the environment are evaluated based on a parametric analysis of the relief, the drainage system, and the texture of the channel. The evaluation of each one of these elements describes the degree of affectation exerted by endogenous and exogenous factors of the earth on them and which, in turn, control the processes of weathering and erosion of the surfaces. From this analysis, the dynamic behavior of each hydrographic basin and its response in qualitative terms of the degree of susceptibility to generating mass movements of the type of landslide, flow, and fall are materialized. For the evaluation of the morphometric conditions present in each of the hydrographic basins, equations arranged internationally for this type of characterizations were used (Table 1). The base cartography was obtained from the free data of the Agustín Codazzi Geographic Institute (IGAC) at a scale of 1:25,000 [42]; in turn, the Digital Elevation Model (DEM) was implemented with a resolution of 12.5 m [43], which was obtained from the portal ASF-ALOS PALSAR. These inputs within the morphometric characterization of the basins are the basis for scale of analysis (1:25,000) and the degree of resolution (12.5 m) of the present study. From the base cartography, the configuration of the drainage network and the altitude levels was obtained, and the limit of the hydrographic basins was defined, as well as other morphometric parameters that will be described below. The concatenation of these two inputs served as the basis for the calculation of each morphometric parameter of the hydrological basins. The morphometric calculations performed were developed on the ArcGIS V10.8 program.

Table 1. Methodology adopted for the calculation of morphometric parameters.

Methods of Calculating Morphometric Parameters			
Morphometric Parameters		**Methods**	**References**
Drainage Network	Area (km^2) (A)	GIS Software	GIS processing
	Perimeter (km) (P)	GIS Software	Schumm [24]
	Relative perimeter (Pr)	Pr = A/P	Schumm [24]
	Basin length (Lb) (km)	GIS Software	Schumm [24]
	Length area relation (Lar)	Lar = 1.4 × $A^{0.6}$	Hack [44]
	Stream order	Hierarchical Rank	Strahler [45]
	Stream number (Nu)	Nu = N1 + N2 . . . + Nn	Horton [46]
	Total stream order	Sum of Stream order	GIS processing
	Total stream length (Lu) (km)	Lu = L1 + L2 . . . + Ln	Strahler [16]
	Bifurcation ratio (Rb)	Rb= Nn/Nn + 1	Strahler [16]
	Form factor (Rf)	Rf = A/Lb^2	Horton [22]
Drainage Texture and Flow Mobility Analysis	Drainage density (Dd)	Dd = Lu/A	Horton [22]
	Stream frequency (Fs)	Fs = Nu/A	Horton [22]
	Drainage texture (T)	T = Dd × Fs	Smith [23]
	Torrential coefficient (Ct)	Ct = Stream order 1/A	Romero Díaz [47]
	Basin concentration time (Tc)	Different equations	References in the text

Table 1. *Cont.*

Methods of Calculating Morphometric Parameters			
Morphometric Parameters		**Methods**	**References**
Relief Characterization	Average height of the basin (Hm)		
	Average slope (°)	GIS Analysis/DEM	GIS processing
	Average slope (%)	GIS Analysis/DEM	GIS processing
	Total basin relief (H) (m)	H = Z-z	Strahler [16]
	Relief ratio (Rhl) (m)	Rhl = H/Lb	Schumm [24]
	Asymmetry factor (Af)	Af = 100 × (Ar/A)	Keller and Pinter [48]
	Hypsometric curve	Area-altitude relates	Strahler [16]
	Compactness coefficient (Kc)	Kc = 0.28 × (P/$\sqrt{A}$)	Gravelius [21]
	Massive coefficient (Cm)	Cm = Hm/A	Martonne [49]
	Orographic coefficient (Co)	Co = ((Hm/1000)^2)/A	Fournier [50]
	Elongation relation (Re)	Re = 1.128 × $\sqrt{A}$/L	Schumm [24]
	Circulatory ratio (Rc)	Rc = 4π × A/P^2	Miller [51]
	Sinuosity of mountain front (Smf)	Smf = Lmf/Ls	Bull and McFadden [25]
	Ruggedness number (Rn)	Rn = Dd × (H/1000)	Patton and Baker [52]
	Melton ruggedness number (MRn)	MRn = H/A$^{0.5}$	Melton [53]
	Stream length–gradient index (SL)	GIS Toolbox	Daniela Piacentini [54]
	Reason for valley width and valley height (Vf)	Vf = 2Vfw/[(Eld-Esc) + (Erd-Esc)]	Keller and Pinter [48]

The Form factor (Rf) expresses the relationship between the area of the basin (km^2) and the length of the basin (km) [22]. The form factor described by Pérez [55] was used for the evaluation of this parameter. The Drainage density (Dd) parameter indicates the relationship between the total length of the irregular and regular watercourses of the basin (km) and the total area of the basin (km^2) [22]. This parameter provides a real measure of drainage efficiency when examining the capacity to dislodge a volume of water. The Drainage Texture (T) parameter shows a relationship between Drainage density (Dd) by Stream frequency (Fs) [23]. This parameter is conditioned by factors such as climate (temperature and precipitation), vegetation, type of rock and soil, infiltration capacity, relief, and its state of development.

The Basin concentration time (Tc) evaluates the hydraulic behavior of each basin against each morphometric and morphological aspect. The concentration time is the travel time of a drop of rainwater that drains superficially from the farthest place in the basin to the point of exit [56]. Different formulas were used to calculate this parameter, which are described below (a–i):

(a) SCS–Ranser method: $T_c = 0.97K^{0.385}$, $K = \frac{L_c^3}{H}$, where T_c is the concentration time (hours), H is the difference between the highest and lowest elevation of the basin (feet) and L_c is the length of the main channel (km) [57].

(b) California Culvert Practice method: $T_c = \left[0.87\frac{L_c^3}{H}\right]^{0.385}$, where T_c is the concentration time (hours), H is the difference between the highest and the lowest level of the basin (m) and L_c is the length of the main channel (km) [58].

(c) Kirpich's method: $T_c = 0.066\left[\frac{L}{\sqrt{S_0}}\right]^{0.77}$, where T_c is the concentration time (hours), L is the length of the main channel to the divide (km) and S_0 is the average slope of the main channel (m/m) [59].

(d) Témez's method: $T_c = 0.3\left[\frac{L_c}{S_0^{0.25}}\right]^{0.76}$, where T_c is the concentration time (hours), L_c is the length of the main channel (km) and S_0 is the average slope of the main channel (in percentage) [60].

(e) Giandotti's method: $T_c = \frac{4\sqrt{A}+1.5L_C}{25.3\sqrt{L_C S_0}}$, where T_c is the concentration time (hours), L_c is the length of the main channel (km), S_0 is the average slope of the main channel (m/m) and A is the area of the basin (km^2) [61].

(f) V.T Chow's method: $T_c = 0.8773\left[\frac{L_c^{1.5}}{\sqrt{CM-Cm_c}}\right]^{0.64}$, where T_c is the concentration time (hours), L_c is the length of the main channel (km), CM is the highest bound of the main channel (m.a.s.l.) and Cm_c is the lowest bound of the main channel (m.a.s.l.) [56].

(g) Clark's method: $T_c = 0.335\left[\frac{A}{S_0^{0.5}}\right]^{0.593}$, where T_c is the concentration time (hours), S_0 is the average slope of the main channel (m/m) and A is the area of the basin (km^2) [62].

(h) Ventura–Heron method: $T_c = 0.3\left[\frac{L_c}{S_0^{0.25}}\right]^{0.75}$, where T_c is the concentration time (hours), L_c is the length of the main channel (km) and S_0 is the average slope of the main channel (in percentage) [63].

(i) Passini's method: $T_c = 0.108\frac{(AL_C)^{1/3}}{\sqrt{S_0}}$, where T_c is the concentration time (hours), L_c is the length of the main channel (km), S_0 is the average slope of the main channel (m/m) and A is the area of the basin (km^2) [64].

The parameter Asymmetry factor (Af) describes tectonic tilting conditions perpendicular to the main drainage direction. It is defined by the basin area to the right of the main drainage downstream (Ar) and the total basin area (A) [48]. Depending on its result, a tilt is defined to the left (>50) or to the right (<50). The Compactness coefficient (Kc) compares the shape of the basin with that of a circumference whose inscribed circle has the same area of the basin under study. It is defined with the perimeter of the basin and the area of the basin. The degree of approximation of this index to the unit will indicate the tendency to concentrate strong volumes of runoff water, being more accentuated the closer it is to the index, that is, the greater the concentration of water [21]. The Massive coefficient (Cm) calculates the condition of the basin with respect to whether it is mountainous or, on the contrary, a flat basin [49].

The Orographic coefficient (Co) parameter expresses the degradation potential of the basin and considers the average height of the basin which directly influences the potential flow of water and the area whose inclination exerts direct action on surface runoff [50]. The result expresses a little rugged relief for <6 values, as well as extensive basin, low slope, and lower erosion, and for >6 values, it expresses a rugged relief with a high degree of erosion [50]. The Elongation relation (Re) is described as the quotient between the diameter of a circle with the same basin surface area and the maximum length of the basin, defined as the largest dimension of the basin, along a straight line from the outlet to the extreme boundary of the watershed, parallel to the main river [24]. The Circularity ratio (Rc) shows the relationship between the basin area and the circle area with the same circumference as the basin perimeter. This relationship is influenced by current length and frequency, geological structure, land use and/or land cover, climate, and slope [51].

The Sinuosity of mountain front (Smf) parameter is defined as the ratio or relationship between the total length of the mountain front (Lmf) and the straight-line length measured between the ends of the mountain front (Ls) [25]. The Index of the gradient of the longitudinal profile of the riverbed (SL) is used to detect the anomalous gradients within the path of the currents in a hydrographic basin from the morphometric point of view [65]. The drainage network presents regular geometric properties which establish erosive processes that help provide data on the geological conditions of the evaluated area as well as its geomorphological evolution [66]. The parameter of Reason for valley width and valley height (Vf), according to Bull and McFadden, (1977); Bull, (1978); cited in Keller and Pinter [48], allows to evaluate the distribution and degree of tectonic activity specifically on the mountain range–piedmont junction. This parameter differentiates between broad-based valleys with relatively high values that indicate degradation processes and low rates of uplift, and valleys in the form of "V" with relatively low values that suggest prolonged incision and active lifting. The equation defines the Reason for valley width and valley

height (Vf), where the average height of the slope on the left side of the valley is Eld, the average height of the left side is Erd, the measure of elevation of the channel is Esc, and the width of the valley is Vfw.

5. Results

From the morphometric analysis carried out on each hydrographic basin following the proposed methodology and the equations described above, each morphometric aspect was determined as a regional evaluation. The following results are obtained from this analysis.

The Form factor parameter (Rf) described by Horton [22] determined that the hydrographic basins of Río Negro, Río Guaca, river and Seca, Felisco and El Abra stream have a slightly elongated geometry (northeast region) providing conditions of moderate to low occurrence to sudden floods of the channels. On the other hand, the basin of the Cantabara stream (widened geometry) has a greater tendency to generate a sudden flood of the channel (Table 2).

The Bifurcatio ratio (Rb) parameter describes the change ratio of each drainage order [16]. This relationship shows that the Calichana stream–Seca stream (Rb, orders 1 and 2), Las Pavas stream–Perchiquez stream (Rb, orders 2 and 3), Chorrerana stream–Perchiquez stream (Rb, order 3 and 4) and Manco River–Umpalá River (Rb, order 4 and 5) present the highest Rb coefficients due to an orographic factor that is controlled by the geological conditions associated with the stroke of the Bucaramanga fault line, Perchiquez and Umpalá faults that affect rocks especially of Precambrian (PD) and Jurassic (J) age causing their steep terrains that generate very erodible soils (Table 2).

Performing a comprehensive analysis of the parameters calculated in Table 2 for the description of the drainage network, it is determined that the basins of the Guaca, Umpalá and Manco rivers together with the Cantabara, La Cureña and Chorrerana streams present scenarios conducive to the creation of torrential flows, as well as weathering processes and erosion of their surfaces, giving rise to a high concentration of stone material especially of rocks of Precambrian (PD) and Jurassic (J) origin.

Within the parameters for the characterization of the relief of the hydrographic basins, the Asymmetry factor (Af) describes a tendency of the basins to tilt to the right with a marked asymmetry. The basins with the highest Af coefficients are Umpalá, Quebrada Seca and Quebrada Talarcuta. This tilting factor is controlled by tectonic and structural conditions, especially by the stroke of the Bucaramanga fault, that present kinematics of sinistral course with a reverse component (Figure 4 and Table 3). The Compactness coefficient (Kc) signifies that the Cantabara, Felisco streams and the Río Negro River have a round-oval to oblong-oval basin shapes with indices closer to 1, indicating the tendency to concentrate strong volumes of water by runoff from their surfaces. The Massive coefficient (Cm) describes a tendency of the basins towards a mountainous to very mountainous relief, the streams El Abra, Seca and Las Pavas being the surfaces that present the highest coefficients in this parameter (Table 3).

The parameter of Orographic coefficient (Co) presents a similar behavior for all basins, with little rugged reliefs, extensive basins, low slope, and less erosion (Table 3). The elongation ratio (Re) describes a tendency towards elongated to very elongated basins, with the Manco River and the Talarcuta and Perchiquez streams having the lowest indices (Table 3). In turn, this parameter indicates a delay in the concentration of runoff due to the length of the channel, which generates a high probability of torrential flow when the channel reaches its maximum concentration level [67]. The Circularity ratio (Rc) also defines the ability of the basin to evacuate runoff water. This parameter is based on the area of the basin. The coefficients obtained show a tendency towards intermediate to slightly elongated basins. The basins with lowest coefficients are the Manco River and the Perchiquez and Talarcuta streams, which will have a delay in runoff concentration due to the length of the channel (Table 3).

Table 2. Morphometric parameters calculated for all basins. Drainage network.

Basin	Area (km^2) (A)	Perimeter (km) (P)	Relative Perimeter (Pr)	Basin Length (Lb) (km)	Length Area Relation (Lar)	Stream Order (max.)	Total Stream Order	Total Stream Length (Lu) (km)	Bifurcation Ratio (Rb)					Form Factor (Rf)
									1–2	2–3	3–4	4–5	5–6	
Umpalá River	205.58	86.27	2.38	30.19	34.19	5	881	663.90	3.9	4.9	3.5	10.0	-	Elongated (0.23)
Río Negro River	91.91	45.36	2.03	16.22	21.09	5	230	245.84	3.6	3.5	4.3	3.0	-	Slightly elongated (0.35)
Manco River	140.16	83.59	1.68	31.10	27.17	5	732	522.51	3.8	4.1	3.2	11.0	-	Very elongated (0.14)
Guaca River	529.52	123.82	4.28	40.69	60.32	6	1707	1524.53	4.0	3.2	3.2	5.0	6.0	Slightly elongated (0.32)
Talarcuta stream	39.11	37.79	1.03	15.30	12.63	5	270	168.75	4.8	4.4	2.5	4.0	-	Very elongated (0.17)
Seca stream	3.24	8.98	0.36	3.03	2.84	4	60	21.04	5.9	2.0	4.0	-	-	Slightly elongated (0.35)
Perchiquez stream	82.90	56.90	1.46	21.44	19.83	5	415	293.82	3.4	5.9	5.0	3.0	-	Very elongated (0.18)
Las Lauchas stream	24.69	26.31	0.94	9.86	9.59	5	180	121.32	3.9	2.4	3.5	4.0	-	Elongated (0.25)
La Cureña stream	19.43	21.56	0.90	6.98	8.30	5	81	63.42	2.4	5.5	2.0	2.0	-	Neither elongated nor widened (0.4)
La Basteña stream	23.04	23.17	0.99	8.93	9.20	5	201	117.15	4.1	3.0	4.0	3.0	-	Elongated (0.29)
Felisco stream	13.25	17.07	0.78	6.08	6.60	4	125	69.89	4.7	4.2	5.0	-	-	Slightly elongated (0.36)
El Abra stream	3.79	9.27	0.41	3.29	3.11	4	43	22.40	3.9	2.7	3.0	-	-	Slightly elongated (0.35)
Las Pavas stream	9.47	15.82	0.60	5.77	5.39	4	82	46.66	3.9	8.0	2.0	-	-	Elongated (0.28)
Chorrerana stream	18.16	20.48	0.89	6.87	7.97	4	62	48.51	2.6	2.1	7.0	-	-	Neither elongated nor widened (0.39)
Cantabara stream	52.03	32.84	1.58	9.23	14.99	5	248	189.20	4.9	3.3	3.0	4.0	-	Widened (0.61)
Calichana stream	12.83	16.96	0.76	5.47	6.47	4	75	85.77	6.1	3.3	3.0	-	-	Neither elongated nor widened (0.43)

The green box indicates the quantitative valuation in a low range for this parameter. The red box indicates the quantitative valuation in a high range for this parameter.

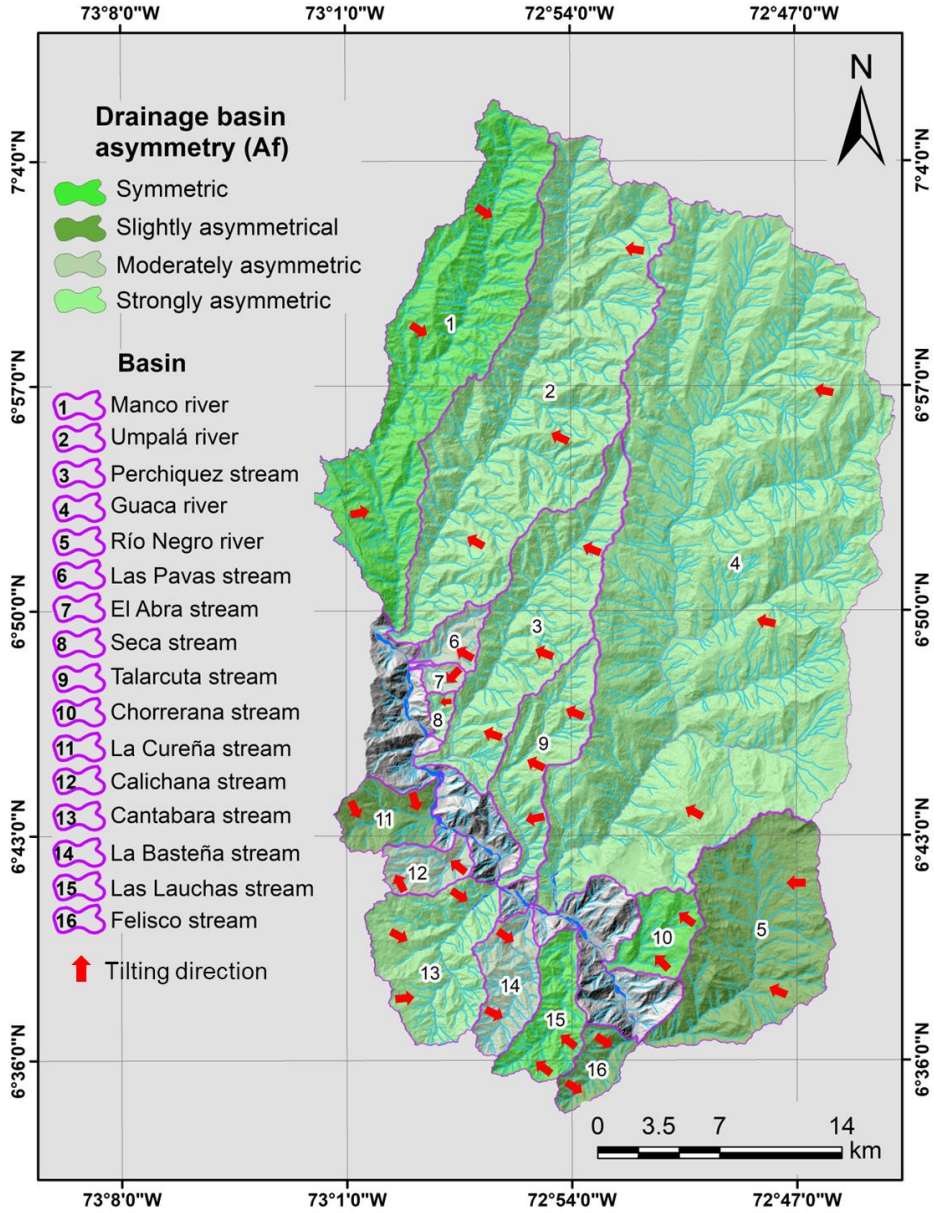

Figure 4. Morphometric parameter of asymmetry of the basins (Af).

For the parameter of Sinuosity of mountain front (Smf) it is observed that a large part of the basins is in an active state, except for the basins of the La Cureña, Seca, Cantabara and Calichana streams (little activity). The basins of the Chorrerana, Perchiquez and Talarcuta streams show very low coefficients that indicate greater activity of the mountain front in weathering processes and erosion of the rocky massif (Figure 5 and Table 3).

The hypsometric curve is one of the most important parameters in the morphometric assessment of the basins due to its relationship with the state of erosion of the channel. To carry out the analysis of all the basins, a normalization of the data was carried out, superimposing the trends of all the basins. Within the construction of the curves and their interpretation, the mature state (red line) was considered as the basis for the graphic output (Figure 6).

With the construction and evaluation of the hypsometric curves, three conditions are described: (1) basins in juvenile state, where there is great potential for erosion (bottom undermining of the bed), (2) basins in mature state, where there is balance (bottom and lateral undermining), and (3) basins in senile state, where lateral deposition and undermining conditions occur [45]. With these conditions, it is observed that the basins present in

the northern region (right bank, downstream of Chicamocha River) mostly have Condition 2, except Río Negro and Guaca rivers (Condition 1) and Quebrada Seca (Condition 3). The basins present in the southern region (left bank, downstream of Chicamocha River) such as Felisco, Basteña and Calichana streams have Condition 1, Cantabara and Lauchas streams present a transition phase between Conditions 1 and 2, and Cureña stream is in Condition 2. This shows that a large part of the basins is in the process of deepening to reach a channel balance.

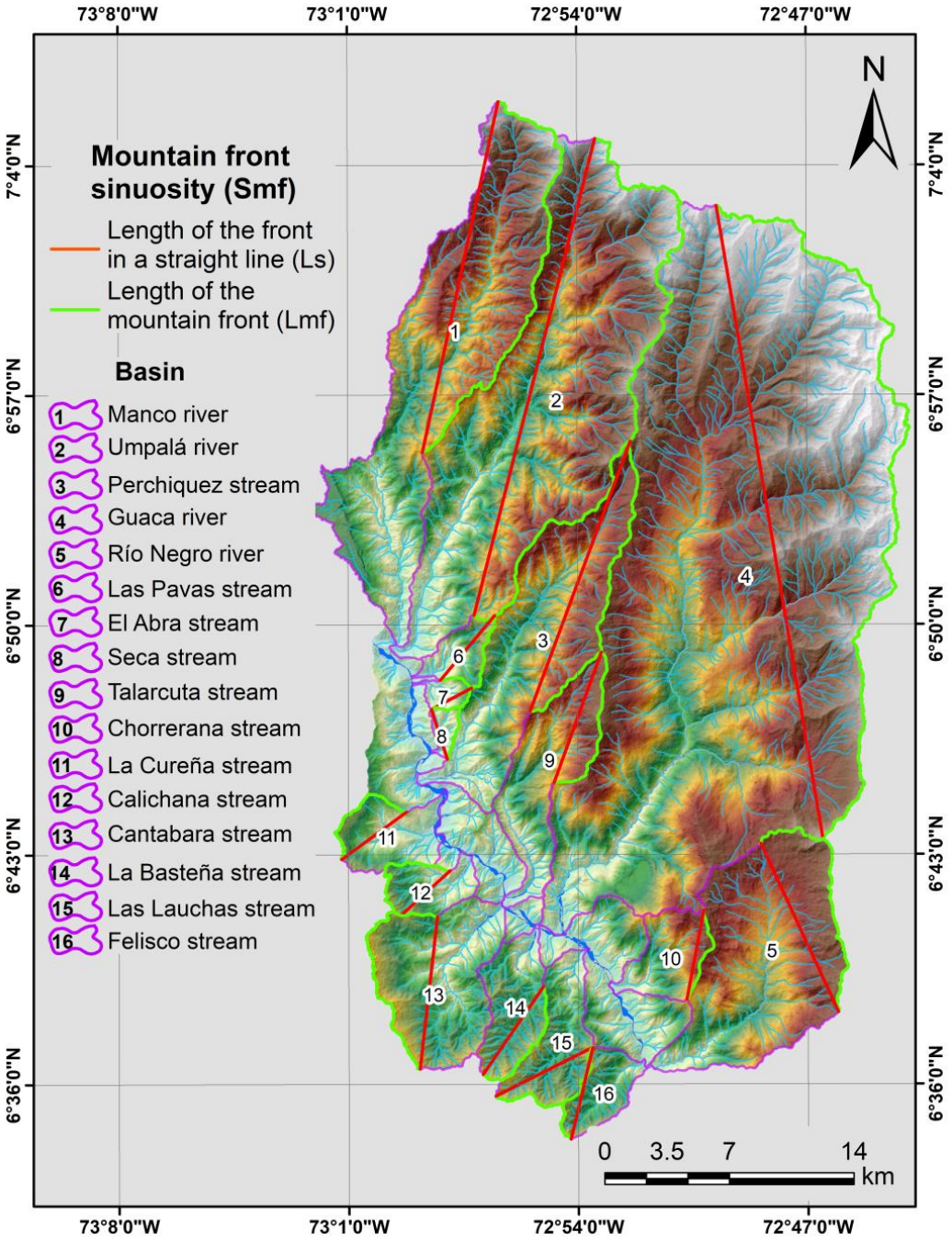

Figure 5. Sinuosity of the mountain front (Smf).

Table 3. Morphometric parameters calculated for all basins. Relief characterization.

Basin	Average Height of the Basin (m)	Average Slope (°)	Average Slope (%)	Total Basin Relief (H) (m)	Relief Ratio (Rhl) (m)	Asymmetry Factor (Af)	Compactness Coefficient (Kc)	Massive Coefficient (Cm)	Orographic Coefficient (Co)	Elongation Relation (Re)	Circulatory Ratio (Rc)	Sinuosity of Mountain Front (Smf)	Ruggedness Number (Rn)	Melton Ruggedness Number (MRn)
Umpalá River	2321.49	31.36	63.96	3477.00	115.19	25.86	1.70	11.29	0.08	0.54	0.35	1.50	11.23	0.24
Río Negro River	2369.52	23.08	45.00	2826.00	174.27	44.76	1.33	25.78	0.19	0.67	0.56	1.50	7.56	0.29
Manco River	2139.88	26.74	52.80	3357.00	107.93	50.29	1.99	15.27	0.11	0.43	0.25	1.37	12.51	0.28
Guaca River	2815.29	23.83	46.68	3750.00	92.16	32.66	1.52	5.32	0.04	0.64	0.43	1.41	10.80	0.16
Talarcuta stream	1963.93	29.68	59.67	2629.00	171.88	32.54	1.70	50.22	0.37	0.46	0.34	1.22	11.34	0.42
Seca stream	895.32	29.72	58.99	923.00	304.90	26.99	1.41	276.21	2.04	0.67	0.51	1.67	5.99	0.51
Perchiquez stream	2026.94	30.12	61.04	2789.00	130.07	34.06	1.76	24.45	0.18	0.48	0.32	1.17	9.88	0.31
Las Lauchas stream	1609.22	27.57	53.89	1447.00	146.73	53.91	1.49	65.17	0.48	0.57	0.45	1.43	7.11	0.29
La Cureña stream	1254.66	25.29	48.70	1414.00	202.64	43.48	1.38	64.58	0.48	0.71	0.53	1.65	4.62	0.32
La Basteña stream	1577.34	27.39	53.79	1458.00	163.19	39.85	1.36	68.45	0.51	0.61	0.54	1.28	7.41	0.30
Felisco stream	1601.00	30.49	60.88	1359.00	223.39	40.96	1.32	120.85	0.89	0.67	0.57	1.26	7.17	0.37
El Abra stream	1097.79	29.52	58.48	1150.00	349.16	64.83	1.34	289.87	2.14	0.67	0.55	1.22	6.80	0.59
Las Pavas stream	1379.42	31.13	63.12	1663.00	288.38	38.56	1.45	145.72	1.08	0.60	0.48	1.46	8.20	0.54
Chorrerana stream	1948.34	30.72	62.80	2318.00	337.60	46.81	1.36	107.31	0.79	0.70	0.54	1.13	6.19	0.54
Cantabara stream	1530.51	27.20	53.30	1595.00	172.86	34.69	1.28	29.41	0.22	0.88	0.61	1.71	5.80	0.22
Calichana stream	1361.16	28.12	54.90	1449.00	265.08	60.60	1.34	106.07	0.78	0.74	0.56	2.10	9.68	0.40

The green box indicates the quantitative valuation in a low range for this parameter. The red box indicates the quantitative valuation in a high range for this parameter.

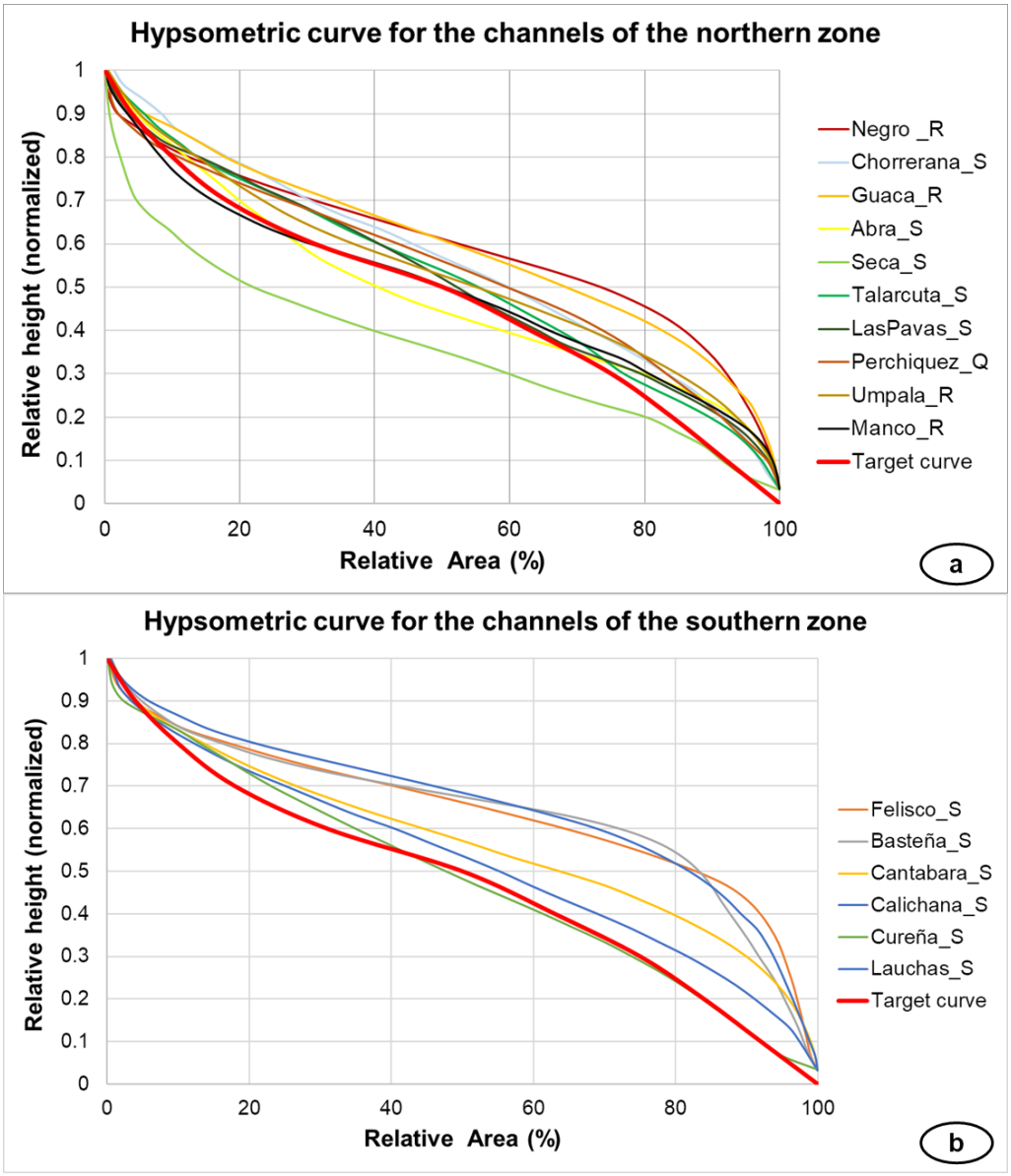

Figure 6. (**a**) Hypsometric curves for the northern region. (**b**) Hypsometric curves for the southern region. The red line indicates (mature state) the basis for the analysis of hypsometric behavior.

The Index parameter of the gradient of the longitudinal profile of the river channel (SL) or Hack Index parameter quantifies the geomorphological conditions within the causes (peaks in erosion dynamics) that have been affected by tectonic activity, differential erosion of rocks and slope instability processes. Its implementation in this type of studies helps to detect knickzones which are the turning points on the longitudinal profile of the current (typical shape: concave upwards) [54]. As a result of this analysis, active processes of the slopes (landslides) that can interact directly with the riverbed can be described, as well as the presence of geological structures and affectation of the shape of the channels [54] (Figure 7).

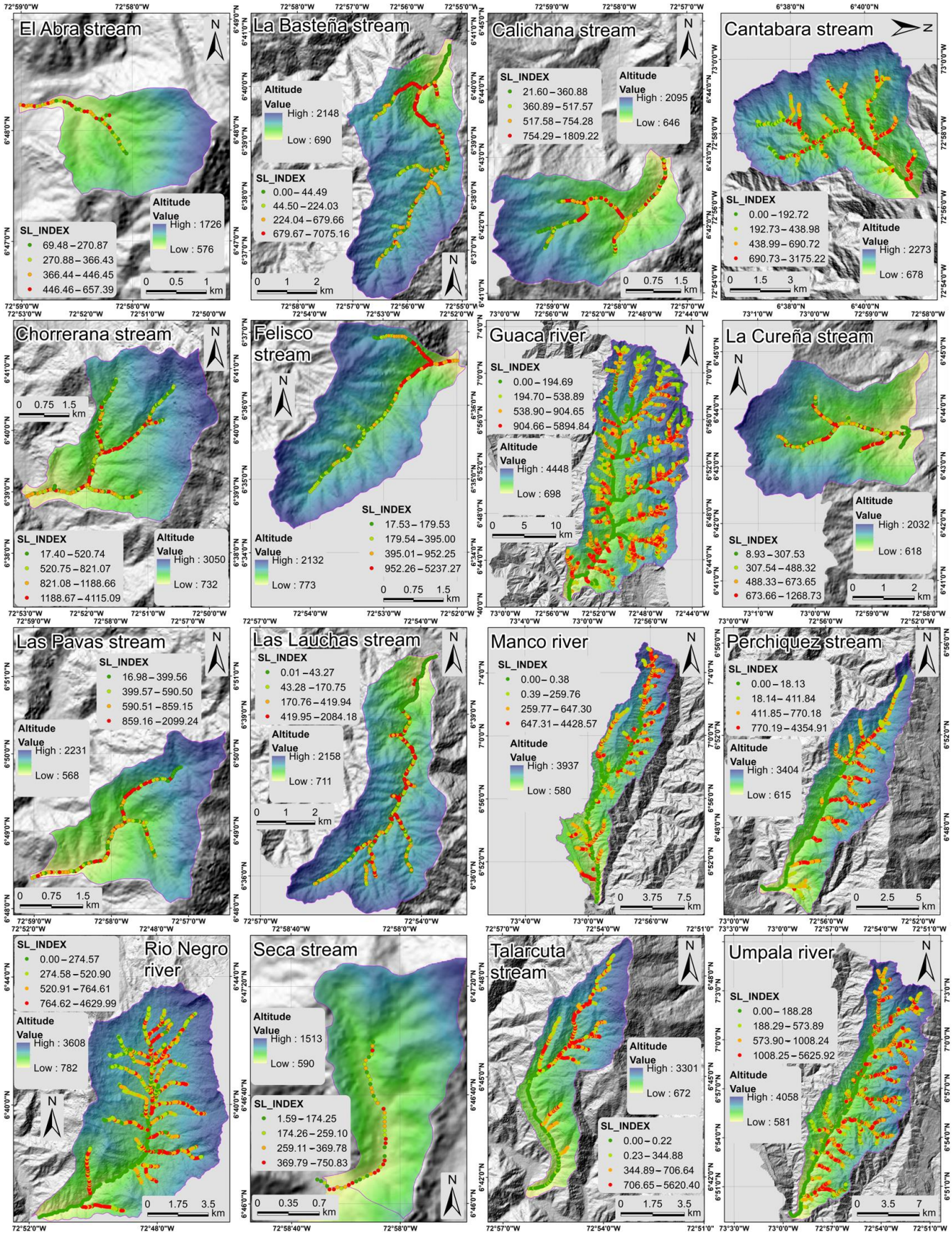

Figure 7. Index of the gradient of the longitudinal profile of the riverbed (SL) for each of the hydrographic basins.

Considering the above, it is determined that

1. The Manco River has the largest number of knickzones towards the upper part of the basin. It is related to a slope change and altitudinal difference. Due to high concentration of knickzones in this part of the basin, it is more susceptible to generate processes of erosion of the channel that can trigger events of the type of torrential flows.
2. Umpalá River presents on its tributaries on the left bank (downstream) a high concentration of knickzones. This may be related to the stroke of Umpalá Fault and the tilting present in the basin.
3. Guaca River presents a condition like that of Umpalá River, with the exception that the knickzones are concentrated in the upper parts of each tributary.
4. The Rio Negro basin presents knickzones in several segments of the river, upper part of the basin, tributaries of the left surface (downstream) and the lower zone of the basin. It can be mainly related to the stroke of the Bucaramanga fault, in addition to multiple structures and lithologies present in the area.
5. The Perchiquez stream basin has the same condition as that of the Umpalá, and the Talarcuta stream basin has a higher concentration of knickzones in the region of change in course of drainage. This change in direction and concentration of knickzones is associated with the stroke and kinematics of the Bucaramanga Fault.
6. The other basins present on the right bank of Chicamocha River (downstream), such as the Seca, Chorrerana, Abra and Pavas streams, present a greater number of knickzones in the middle part of the basins. This is associated with a structural behavior (mainly the Bucaramanga fault), altitudinal difference and lithological change.
7. The basins of the Calichana, Cantabara, Felisco, Cureña, Lauchas and Basteña streams (left bank of the Chicamocha River) have the highest concentration of knickzones in the middle part of each basin. These knickzones are associated with the structural behavior of the Bucaramanga fault, together with an altitudinal difference.

The conditions evaluated by this morphometric parameter show areas of sectorized concentration described above, which indicates the regions highly susceptible to erosion processes (lateral and vertical) that are controlled by structural aspects, exerted mainly by the Bucaramanga fault stroke, as well as lithological aspects, since almost 50% of the rocks are of igneous and metamorphic origin, causing rigidity of the rocky massif. Added to these conditions are the physical characteristics of the environment described in Tables 2 and 3, as well as the tilting of the basins as currently reflected on the shape of the landscape. In some sectors, torrential flows can be generated by the combination of two or more conditions described.

Within the evaluation of the characterization of the relief of the hydrographic basins, the parameter of Drainage density (Dd), Horton [22] defines the efficiency of drainage on the basis of whether a basin can dislodge a volume of water in the shortest possible time. Within this parameter it is described that the basins of the Río Negro, Río Guaca, Río Umpalá, the Chorrerana, La Cureña and Perchiquez streams present a moderate to low drainage density, which indicates a greater time required to dislodge the volume of water contained in the hydrographic basin (Table 4).

Table 4. Morphometric parameters calculated for all basins. Drainage texture and flow mobility analysis.

Basin	Drainage Density (Dd)	Stream Frequency (Fs)	Drainage Texture (T)	Torrential Coefficient (Ct)	Basin Concentration Time. Methods (Result in Hours)									
					Scs-Ranser	California Culvert Practice (1942)	Kirpich (1942)	Témez (1978)	Giandotti	V.T Chow	Clark	Ventura-Heron (1949)	Passini	Average
Umpalá River	3.23	4.29	13.84	3.23	1.36	2.10	1.08	1.81	0.92	1.70	2.30	1.77	2.48	1.73
Río Negro River	2.67	2.50	6.69	1.82	0.72	1.11	0.77	1.21	0.92	1.00	1.58	1.19	1.84	1.15
Manco River	3.73	5.22	19.47	3.87	1.43	2.20	1.19	1.92	0.92	1.77	1.94	1.88	2.43	1.74
Guaca River	2.88	3.22	9.28	2.38	1.87	2.88	1.54	2.42	1.39	2.21	4.42	2.35	4.40	2.61
Talarcuta stream	4.31	6.90	29.79	5.40	0.69	1.07	0.66	1.10	0.63	0.97	0.88	1.08	1.18	0.92
Seca stream	6.49	18.51	120.12	14.50	0.16	0.25	0.19	0.32	0.35	0.29	0.20	0.32	0.30	0.26
Perchiquez stream	3.54	5.01	17.74	3.70	1.00	1.54	0.85	1.41	0.75	1.31	1.36	1.38	1.67	1.25
Las Lauchas stream	4.91	7.29	35.82	5.18	0.52	0.81	0.49	0.80	0.59	0.77	0.69	0.79	0.92	0.71
La Cureña stream	3.26	4.17	13.61	2.68	0.35	0.55	0.39	0.63	0.60	0.56	0.61	0.62	0.79	0.57
La Basteña stream	5.08	8.72	44.34	6.47	0.47	0.72	0.45	0.74	0.59	0.70	0.66	0.73	0.87	0.66
Felisco stream	5.28	9.44	49.78	7.40	0.31	0.47	0.32	0.54	0.49	0.49	0.46	0.54	0.60	0.47
El Abra stream	5.91	11.35	67.15	8.19	0.16	0.25	0.20	0.34	0.36	0.29	0.22	0.34	0.33	0.28
Las Pavas stream	4.93	8.66	42.70	6.66	0.27	0.41	0.30	0.52	0.43	0.44	0.37	0.51	0.52	0.42
Chorrerana stream	2.67	3.41	9.12	2.15	0.29	0.44	0.35	0.59	0.52	0.47	0.55	0.59	0.68	0.50
Cantabara stream	3.64	4.77	17.33	3.69	0.47	0.72	0.47	0.76	0.76	0.70	1.07	0.75	1.16	0.76
Calichana stream	6.68	5.84	39.06	4.75	0.26	0.41	0.31	0.51	0.51	0.44	0.46	0.51	0.60	0.45

The green box indicates the quantitative valuation in a low range for this parameter. The red box indicates the quantitative valuation in a high range for this parameter.

The Drainage texture (T) defines the level of runoff that a basin can have [23]. From this parameter, it was determined that 70% of the basins (11 basins) present a very fine drainage texture, indicating basins with high levels of surface runoff, impermeable rock massif and low permeability soils. The Río Negro, Río Guaca and Quebrada Chorrerana basins present an intermediate texture, characteristic for areas with medium runoff levels, with an intermediate texture and permeability of soils (Table 4). For parameter of Reason for valley width and valley height (Vf), it was observed that the basins of the Manco, Río Negro and Umpalá, and the Calichana, Cantabara, La Cureña, Perchiquez and Talarcuta streams in some sectors of the channel present strong processes of incision and lifting with active fronts. The other basins including those previously named display degradation conditions, with expansion of the bottom and inactive front. The Ruggedness number (Rn) parameter indicates the structural complexity of the terrain associated with relief and drainage density [52]. The result of Rn indicates that the Manco, Talarcuta Umpalá, and Guaca basins have a high structural complexity and are very susceptible to high erosion of their surfaces. On the contrary, the Chorrerana, Seca, Cantabara, and La Cureña basins have the lowest coefficients. Finally, the Melton ruggedness number (MRn) shows the index related to the accumulation and resistance of the simple flow of a basin, which, in turn, describes the susceptibility to generate different types of flow [53]. From the result of MRn, it is interpreted that the basins La Basteña, Río Negro, Las Lauchas, Manco, Umpalá, Cantabara, and Guaca are prone to generate flows with low material content. The Seca, Talarcuta, Calichana, Felisco, La Cureña, and Perchiquez basins are prone to generate flows with moderate material content and the El Abra, Chorrerana, and Las Pavas basins are prone to generate flows with high material content.

With the results obtained from Tables 3 and 4, an integral analysis of these twelve parameters described for the characterization of the relief was carried out. From this analysis, it was determined that the Manco, Umpalá, Río Negro River basins and the Talarcuta and Perchiquez streams present the most unique conditions within each evaluation carried out. From the calculation of each parameter, a control is observed by processes of tectonic, structural, lithological and topographic type that provide their own and accentuated conditions in sectors within each of these hydrographic basins. The combination of each of these elements magnifies the processes of erosion of the rock mass and of the channels, giving rise to processes of lateral and vertical erosion of the channel that, together with the speed in the accumulation of the flow, result in a favorable scenario for torrential flow type events.

Within the parameters for the analysis of the flow mobility of the hydrographic basins, the Torrential coefficient (Ct) was evaluated. From this parameter, it can be seen that the basins of the Las Pavas, Felisco, El Abra and Seca streams have the highest torrential indices. On the other hand, the basins of the Guaca, Río Negro rivers and the Chorrerana and La Cureña streams present the lowest indices. Finally, the Basin concentration time (Tc) of each basin was estimated. From the results obtained, it can be seen that the basins of the Guaca (154.46 min), Manco (104.52 min), Umpalá (103.54 min) and Perchiquez streams (75.17 min) present the highest concentration times (the values present here correspond to the average of the results for each method). The basins of the Seca (15.80 min), El Abra (16.65 min), Las Pavas (25.16 min) and Calichana (26.75 min) streams present the lowest concentration times. At the same time, it is observed that the Manco River basin has an irregular dispersion of the data. This is associated with the geometry of the basin and its structural control (Table 4 and Figure 8a). For Figure 8b, there is a correlation between the concentration times of the basins and the torrential coefficient. From this correlation, it is observed that the basins of the Seca, Felisco, El Abra and Las Pavas streams show low concentration times but the highest rates of torrentiality. This is because they are smaller basins that are in an equilibrium phase (juvenile–mature) where the development of their surfaces generates both vertical and horizontal erosion processes; in turn, a structural control is included that is exerted on these basins, causing significant changes in their surfaces since they are located on the stroke of the Bucaramanga fault.

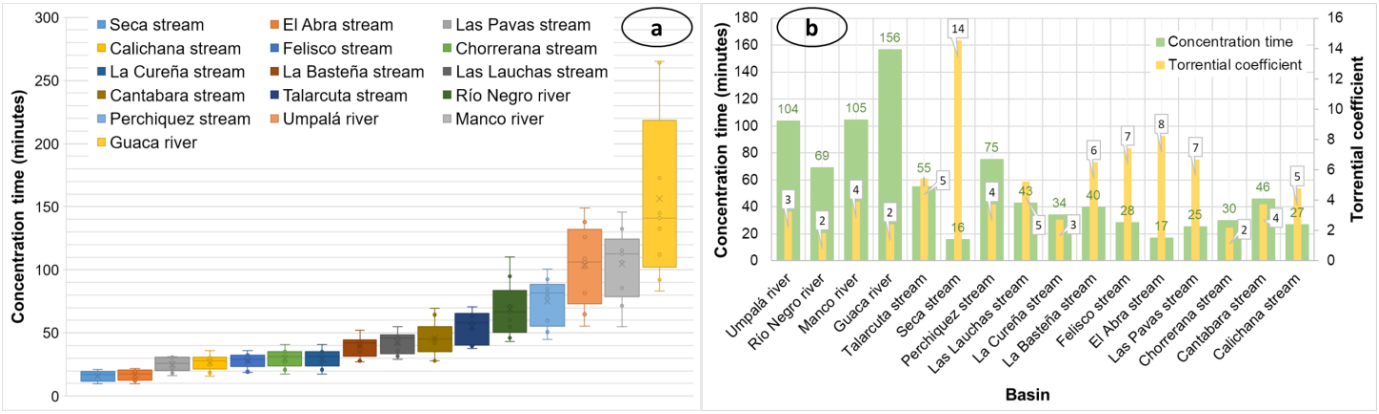

Figure 8. (**a**) Statistical estimation of Basin concentration time (Tc) for each of the equations described. Time in minutes. (**b**) Correlation between concentration times and torrential coefficient.

6. Discussion

With the results obtained in each of the parameters raised, very relevant aspects were detected when performing an evaluation of the geodynamic behavior present for the study region from the point of view of weathering and erosion processes. Within the analyses, it was observed that the morphometric conditions (geometry and surface contrasts) would be strongly controlled by a structural context as described in Tables 3 and 4. The action of regional and local faults such as Bucaramanga, Manco, Umpalá, Perchiquez, Baraya and Morro de las Peña faults create important changes in the surfaces, such as tilting, strong ground incision processes, control in the weathering pattern–erosion, changes in the geomechanical behavior of the rocks and sediment transport. These conditions are represented by the calculations performed with the parameters of the characterization of the relief (Table 3), where basins are described with accentuated processes in the mountain fronts, deepening of the channel due to a phase of dynamic balance of the channels, elongated geometries, tilted and with flexures in the direction of the channels. All these elements together offer a support in the morphometric construction of the landscape that derives in actions at a regional or local level, where the results of the present evaluation serve as a basis input in the ordering of the hydrographic basins. In turn, the descriptions provided by each morphometric parameter define sectors with a greater or lesser degree of affectation by processes that degrade the rocky massif, which provides useful tools in the planning and organization of both natural and physical resources of a territory.

To further understand the development of these basins, regional behavior must be integrated from the tectonic and lithological point of view. The region is located in the tectonic context of the Santander Massif, which is a structure within the eastern mountain range of Colombia. The Santander Massif presents conditions of cortical deformation due to lifting processes, transpressive and elapsed events and compressive deformation with folding in sedimentary rocks [39,41]. These aspects create zones with different degrees of deformation within the massif, which give rise to metamorphic rocks of the mylonite augen, mylonite with non-deformed blocks, mylonite with banding and igneous and sedimentary rock with catalysis types [41]. Due to these tectonic and structural conditions, previous studies in the region have identified sections within the Bucaramanga fault that present different levels of stresses and deformation (Villamizar, (2014) and González and Jiménez, (2014) cited by Velandia and Bermúdez, [39]; García-Delgado, et al., [68]). The study region is part of the sector called the Cepita section, which presents a high structural complexity due to the stroke of the Bucaramanga fault that exhumes part of the fragile–ductile crust zone. This description was constructed on the basis of outcrops with identified structures, in addition to the presence of pseudotachylites that served as indicators of this process (Villamizar, (2014) and González and Jiménez, (2014) cited by Velandia and Bermúdez, [39]). In turn, geomorphological ranges of recent tectonic activity were detected,

such as triangular and trapezoidal facets, sealing ridges, pressure peaks, drainage deviation, linear valleys, and drainage control [41].

With this tectonic and structural perspective present in the study region, contrasts are established with the results of the calculated parameters. Parameters such as the Asymmetry factor (Fa), Hypsometric curve, Massive coefficient (Cm), Orographic coefficient (Co), Sinuosity of mountain front (Smf) and Reason for valley width and valley height (Vf) are closely related to recent tectonic activity. This relationship shows a tendency of tilting of the basins in the direction of stroke and kinematics of the Bucaramanga fault, as expected, except for the basins of Manco River and the Calichana, Las Lauchas and El Abra streams that may be due to a local structural control, a compositional variation of the lithology present or an increase in the rates of weathering and erosion on the surfaces due to zonal climate control. In addition, a relationship is observed between the relief (mountainous to very mountainous) that is a little rugged, with extensive basins, strong processes of incision, lifting, degradation of the slopes, undermining (vertical and horizontal), expansion of the bottom and active fronts that can obey this structural control. In turn, the exhumation rates were recorded by Velandia [69] and Amaya et al. [70] of approximately 0.3 km/Ma from approximately 25 Ma ago. As a parallel process to the exhumation of the rock massif, the weathering of the rocks is generated by pressure relief, where igneous and metamorphic rocks present a decompression by lithostatic load, which produces a fracturing by expansion or dilation of the rocks along the surfaces approximately parallel to the ground [71].

With the approximation performed on the basis of the exhumation rate of the rocky massif, an estimate of the lifting generated in the last 25 Ma is calculated. As a result, it is determined that these surfaces with a constant rate and dynamics for the current period would present a relief of approximately 7500 m. These data contrasted with the current topographic information of the massif for the study area, presenting an altitudinal difference of 3594 m (52.08%). This difference is associated with the degradation of the massif by the action of weathering and erosion processes in the hydrographic basins that are mostly in a juvenile state (hypsometric curve) (Figure 9a). With this result, a statistical modeling (approximation) of the rate of degradation of the massif per million years is carried out, based on the percentage of altitudinal difference and the current volume of the hydrographic basins (Figure 9b).

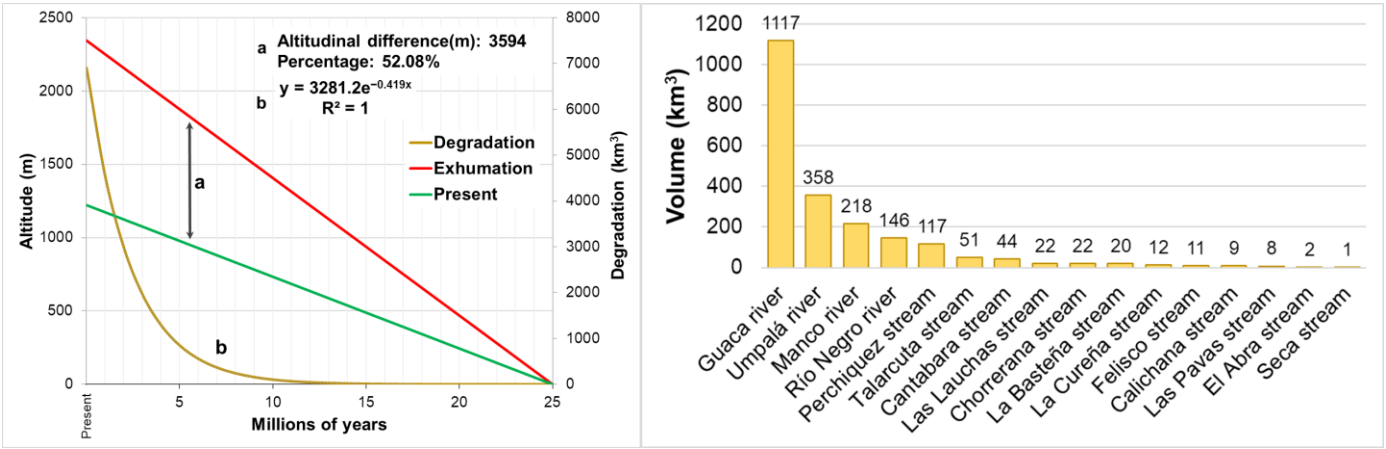

Figure 9. Correlation of exhumation and degradation values of the rock massif. Contrast between the estimate of the solid and the current expression with the degradation curve and current volume of degraded basin area.

Based on the idea that the production of sediments is not proportional to the exhumation rate of the rock massif (non-linear relationship), the behavior of the graph must be expressed exponentially. For a time T_0 (25 Ma ago) production is low, and for a time T_1

(present) it is greater with an increase in degradation per a million years. This is due to the dynamic behavior of the basins and their relationship to the stabilization of the channels due to the lifting. This behavior of degradation of the massif can be explained in a better way based on the equation of the exponential geometric function of population growth proposed by Robert Malthus and adapted for the present research. Since this function shows the conditions of a population that grows annually, it can be extrapolated as a function of degradation of the massif for every million years. The equation is $D(t) = D_0 \times (1 + A)^t$, where $D(t)$ is the degradation as a function of time, D_0 is the value of the degradation at a time T_0, A this is the percentage of altitudinal difference and t is the time in millions of years. The output of this function is displayed in Figure 9.

With the relationship generated in Figure 9 between the lifting of the massif and the degradation curve, a trend of degraded volume of each basin can be obtained. The equation in exponential function described as $y = 3281.2e^{-0.419x}$ estimates the volume of degraded material at any point in a timeline, with potential to estimate the volume in the future if the conditions of the site are not altered; in this case, if the exhumation rate is not altered by terrestrial dynamics.

These combined effects create scenarios with zones of fragile behavior that develop multiple fracturing planes (joints) resulting in a degradation of the rock mass by geomechanical aspects of the rocks. Generally, this behavior is associated with lithological units of igneous and metamorphic type, which display mechanical degradation. This is a factor considered in this study for the weathering and degradation of the rock massif. These processes generate a high production of fragmented stone material that is eroded by hydrogravitational, pluvial and fluvial agents. As a consequence of these processes, planes of instability are developed that give rise to mass movements mainly of the rock flow and fall types of some sectors; these movements give rise to geoforms such as talus cones, dejection cones, channels and alluvial–torrential fans (Figure 10).

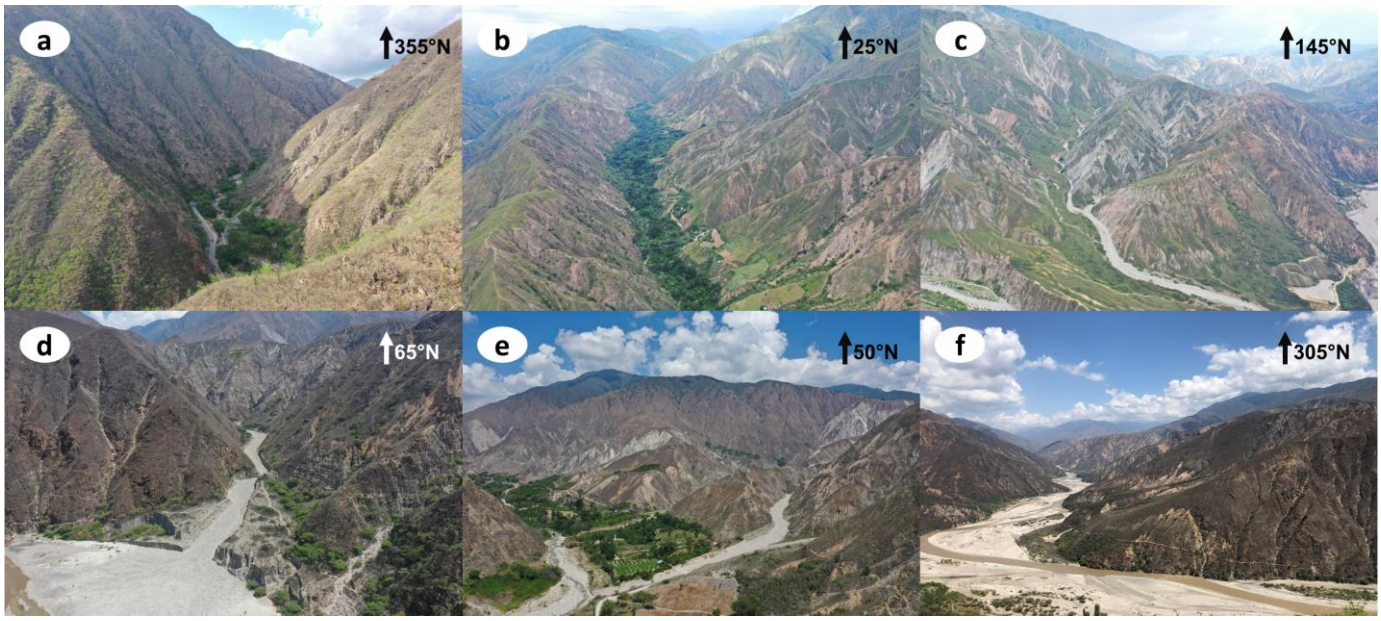

Figure 10. Panoramic image showing the mechanical degradation on the surfaces of several hydrographic basins. Slope movements associated with rock flows can be seen. (**a**) Manco River basin (lower part). (**b**) Umpalá River basin (lower part). (**c**) El Abra stream basin. (**d**) Seca stream basin (lower part). (**e**) Talarcuta stream basin (lower part). (**f**) Chicamocha River heading northwest.

On the other hand, the climatic conditions present in the study region also provide factors that control the rate of degradation of the rocky massif that is consistent with the evolution of the basins and their modeling. For the region, it is described that processes

such as insolation and alternation between wetting and desiccation create constant and progressive states of weathering and erosion. The climate of the Chicamocha Canyon is very exclusive, especially for this region where annual rainfall of 721 mm is recorded with an annual temperature of 25.4 °C. Considering the classification by Thornthwaite [72], this sector of the Chicamocha Canyon basin is described as having a semi-arid climate, without any water gain, and megathermal (DdA'a'). There is no storage of useful water during eleven months of the year (November to September) and precipitation is equal to actual evapotranspiration, except in the month of October [73]. This condition is accentuated by the surrounding topographic control that influences the behavior of the rains in quantity and distribution due to the dynamics of the wind that is affected by the relief. These orographic rains are subject to the mountainous reliefs that serve as a shield for the dry air currents that tend to rise, generating dry and warm climates in the lower parts, while in the upper parts they are humid and rainy [74].

With the climatic conditions described above, weathering processes of the accentuated insolation type are created due to a systematic repetition of the phenomenon of heating of the surfaces, causing a stress that leads to the rupture of the rocks (Figure 11). As a result of this process, a cataphyllar exfoliation or concentric desquamation is present together with a series of fissures that, when converged, create planes where the rocks are eroded (rock fragments). The different surface temperatures affect the minerals present in the rocks magnifying the thermal expansion, which creates a condition of repetitive stresses that could cause rupture by fatigue failure on adjacent minerals, especially those with a granitic composition (igneous rocks) [75]. Additionally, the repetitive alternation of wet and dry states in rocks with high clay contents creates disintegration processes due to increased tension stress. This behavior should be expected for the basins located in the eastern region of the study area (basins of Guaca, Río Negro rivers and the Chorrerana stream) since they present lithologies with more clayey compositions.

Figure 11. Weathering by insolation (thermoclasty). (**a**) Concentric scaly. (**b**) Rupture due to fatigue failure.

Of the morphometric parameters calculated, the Form factor (Rf), Drainage density (Dd), Drainage texture (T), Compactness coefficient (Kc), Ruggedness number (Rn), Melton Ruggedness number (MRn), Torrential coefficient (Ct) and Basin concentration time (Tc) are closely related to climatic factors and basin geometry. Two conditions can be extracted from this characterization. The first is associated with the tributaries of the basins present in the areas proximal to the bed of the Chicamocha River, where channeled mass movements of dry flow are evident. These movements are generated by gravitational processes and high-angle slopes, where the eroded material is accumulated at the tipping points of the slopes that subsequently, by sedimentary load, is set in motion, thus creating channeled

dry flows of fragmented material. The second is associated with the upper parts of the basins, where precipitation levels are higher, leading to the generation of critical flows that, when detected with the stone material arranged in the lower parts of the basins, create torrential flows. Depending on the geometry of the basin, the speed, the concentration of the flow and the material transported, these basins present moderate to high conditions in the generation of torrential flows that bring with them an affectation on anthropic elements (houses, roads, bridges, and agricultural areas).

Finally, a factor that would be affecting the control of weathering and erosion of the rocky massif to a lesser extent is seismic activity. The study area is part of one of the regions with the highest seismic activity in the world. According to Richter [76], the sectors with the highest number of seismic events worldwide are defined as "seismic nests". In turn, this high seismic activity must have persistence over time [77]. The seismic nest of Bucaramanga, as this sector is called, presents a high productivity of seismic events. Based on the catalog of the National Seismological Network of Colombia, between the years 1993 and 2021, which has a total of 153,469 events and historical data collected between 1826 and 1992 with a total of 11 events, an estimate of the seismic productivity is made by applying the equation of Gutenberg and Richter [78]. An important fact to consider is that no data processing was carried out in the catalog, such as parametric and non-parametric controls, data standardization, elimination of anomalous points, selection by seismic source and selection of a single magnitude class. This is because it is sought to determine the seismic productivity present in the region as well as the maximum magnitude it reaches and its probability of occurrence (Figure 12).

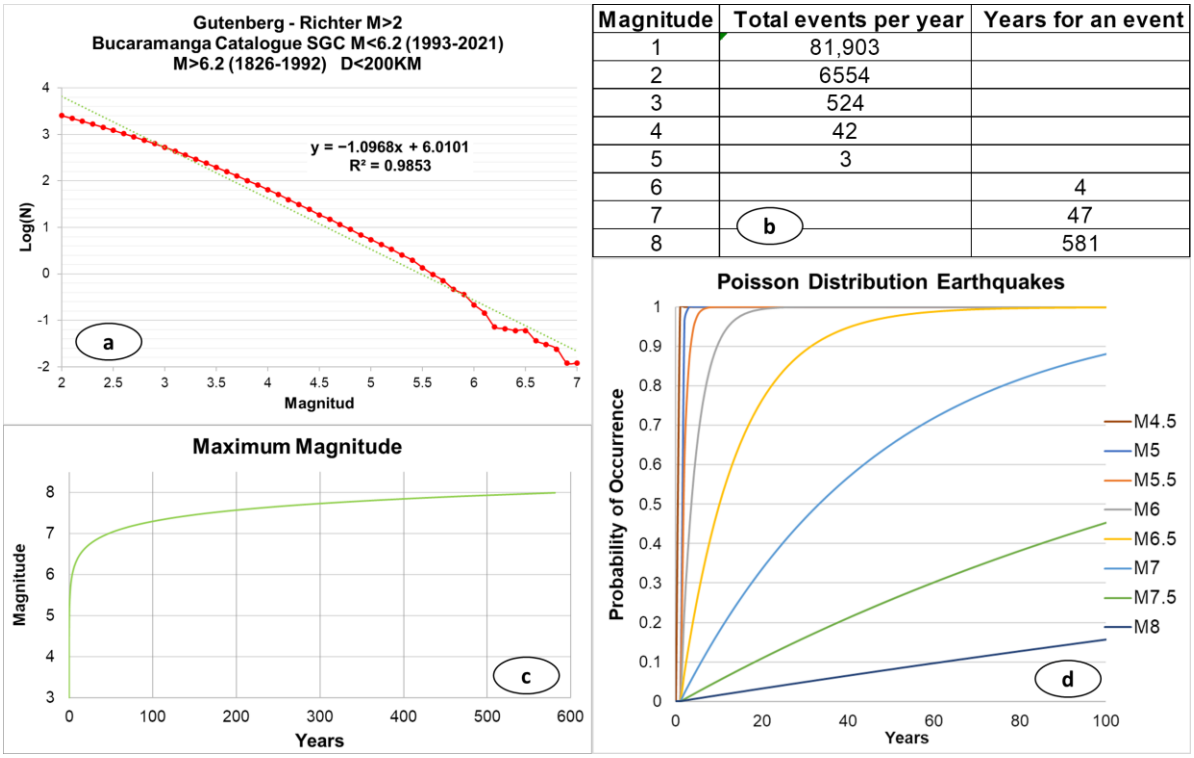

Figure 12. Productivity of the seismic nest of Bucaramanga (evaluation with data from the 1826–1993 "historical catalogue" and the 1993–2021 "new registrations"). (**a**) Linear fit of the Gutenberg–Richter equation by least squares. (**b**) Number of events expected from the solution of the Gutenberg–Richter equation. (**c**) Maximum expected magnitude. (**d**) Poisson distribution that estimates the probability of an event of a certain magnitude occurring.

From the estimation made of seismic productivity, it can be inferred that eighteen events of magnitude 2 or one event of magnitude 3 can be generated in one day. With these

data, a surface scenario can be extrapolated where the rock mass would be in constant excitement due to the vibrations generated in the ground. These vibrations contribute to the processes of mechanical weathering of the rocks creating microcracks that expand by the repeated action of telluric movements. The formation of these microcracks is due to a mechanical induction of the rock massif, which generates a tensional stress that produces cracks caused by local stress that exceeds local resistance [79]. This would be a non-inclusive factor within the dynamic activity of the watersheds, but to some extent would activate the states of weathering and erosion of the rocks due to the constant process of vibration of the rock massif.

7. Conclusions

The present study identified three factors that influence basin modelling, sediment generation and ground instability that give rise to mass movements. The first factor is the most influential and obeys a structural control exercised by the stroke and kinematics of the Bucaramanga fault, where it modifies the geometry, arrangement, and dynamics of the basins, creating planes of weakness that give rise to processes of weathering and accentuated erosion, as well as the generation of slope instability events (rock falls, rock flows and rockslides and/or detritus). The second factor is related to climate control, where the region presents special conditions of temperature, precipitation, and evapotranspiration, giving rise to a dynamic control of the basins, as well as the degradation of the rock massif because of insolation, wetting and drying of the rocks. The combination of the rainy states in the upper parts of the basins, together with the high productivity of sediments in the lower parts, create favorable scenarios for the generation of torrential flows that greatly affect elements of anthropogenic nature. The third factor is focused on the recurring seismic activity in the region. This activity generates rock dislocation processes due to tensional stress, increasing the productivity of rock fragments or contributing to the other two factors in accentuating and magnifying the weathering and mechanical erosion processes present in the region. The combination of the three factors establishes the line of evolution of the landscape present in the region, as well as controls the modeling and the rates of weathering and erosion of the basins, which, in turn, develop the dynamics of the channels that are prone to generating torrential flows.

Within the unified morphometric evaluation of the hydrographic basins, it was observed that the Manco River basin and the Talarcuta, Las Pavas, Felisco and El Abra streams present the geometries, surfaces, and dynamics with the greatest possibilities in the generation of torrential flows. Proof of this is the torrential flow generated by heavy rains over the Manco River basin and its tributaries on 26 February 2020, causing multiple losses of human lives and considerable damage to infrastructure [80]. On the other hand, the basins that present less development to this type of movement are the Umpalá, Guaca, and Río Negro River basins and the Cantabara and La Cureña streams; however, these basins in their lower parts present a high degree of weathering of the rocky massif, giving rise to the formation of hydrogravitational deposits that are arranged on the margins of the channels and provide material for the evolution of torrential flows.

According to the evaluation of the morphometric parameters carried out for all the basins, it is estimated that when heavy or constant rains in the upper parts of the basins are combined with the material arranged by the processes of weathering and erosion that generate deposits in the lower areas of the basins, movements of torrential flow type occur. To some extent, within the evaluation, it is estimated that the development of these movements would be considerably controlled by the amount of rainfall that may occur in the upper parts of the basins. This material is suggested as a reference to consider within the analysis of territorial planning and the use of natural resources.

Author Contributions: Conceptualization, data collection, data analysis, writing draft and final manuscript, J.A.V.O.; concept, writing draft manuscript, A.M.M.-G.; writing of final manuscript, commentary, and revision, J.A.V.O. and A.M.M.-G. All authors have read and agreed to the published version of the manuscript.

Funding: This research received no external funding.

Institutional Review Board Statement: Not applicable.

Informed Consent Statement: Not applicable.

Data Availability Statement: Not applicable.

Acknowledgments: This research was assisted by Project TED2021-131874B-I00 (ATENCACLI) funded by Ministry of Science and Innovation and the GEAPAGE research group (Environmental Geomorphology and Geological Heritage) of the University of Salamanca. The first author thanks the Foundation for the Future of Colombia (COLFUTURO) for the scholarship for doctoral stay. We would like to express our gratitude to Lenny Mejia Mendez for her support bibliographic search, writing and review of the article.

Conflicts of Interest: The authors declare no conflict of interest.

References

1. Intergovernmental Panel on Climate Change (IPCC). Climate change 2007: The Physical Science Basis. In *Contribution of Working Group I to the Fourth Assessment Report of the Intergovernmental Panelon Climate Change*; Solomon, S., Qin, D., Manning, M., Chen, Z., Marquis, M., Averyt, K.B., Tignor, M., Miller, H.L., Eds.; Cambridge University Press: Cambridge, UK, 2007.
2. Gariano, S.L.; Guzzetti, F. Landslides in a changing climate. *Earth Sci. Rev.* **2016**, *162*, 227–252. [CrossRef]
3. Alvioli, M.; Melillo, M.; Guzzetti, F.; Rossi, M.; Palazzi, E.; Hardenberg, J.; Peruccacci, S. Implications of climate change on landslide hazard in Central Italy. *Sci. Total Environ.* **2018**, *630*, 1528–1543. [CrossRef] [PubMed]
4. Patton, A.I.; Rathburn, S.L.; Capps, D.M. Landslide response to climate change in permafrost regions. *Geomorphology* **2019**, *340*, 116–128. [CrossRef]
5. Wood, J.L.; Harrison, S.; Reinhardt, L.; Taylor, F.E. Landslide databases for climate change detection and attribution. *Geomorphology* **2020**, *355*, 107061. [CrossRef]
6. World Health Organization (WHO). Landslides. 2022. Available online: https://www.who.int/health-topics/landslides#tab=tab_1 (accessed on 18 March 2022).
7. EM-DAT. Centre for Research on the Epidemiology of Disasters. Available online: https://www.emdat.be/ (accessed on 25 June 2022).
8. University of Oxford. Our World in Data. Available online: https://ourworldindata.org/grapher/number-of-deaths-from-natural-disasters (accessed on 19 February 2022).
9. Carolyn, K. Informing climate adaptation: A review of the economic costs of natural disasters. *Energy Econ.* **2014**, *46*, 576–592.
10. Cuñado, J.; Ferreira, S. The Macroeconomic Impacts of Natural Disasters: New Evidence from Floods. In *Agricultural and Applied Economics Association's 2011*; Ageconsearch: Pittsburgh, PA, USA, 2011; p. 25.
11. Desinventar. Disaster Information Management System. Available online: https://www.desinventar.org/ (accessed on 30 December 2022).
12. Dávid, L. Quarrying: An anthropogenic geomorphological approach. *Acta Montan. Slovaca* **2008**, *13*, 66–74.
13. Szabó, J.; Dávid, L.; Lóczy, D. *Anthropogenic Geomorphology: A Guide to Man-Made Landforms*; Springer Science & Business Media: Berlin/Heidelberg, Germany, 2010. [CrossRef]
14. Abedini, A.; Calagari, A.A. Geochemistry of claystones of the Ruteh Formation, NW Iran: Implications for provenance, source-area weathering, and paleo-redox conditions. *Neues. Jahrb. Miner. Abh.* **2017**, *194*, 107–123. [CrossRef]
15. Abedini, A.; Khosravi, M. Geochemical constraints on the Zola-Chay river sediments, NW Iran: Implications for provenance and source-area weathering. *Arab. J. Geosci.* **2022**, *15*, 1515. [CrossRef]
16. Strahler, A.N. Part II. Quantitative Geomorphology of Drainage Basins and Channel Networks. In *Handbook of Applied Hydrology*; McGraw-Hill: New York, NY, USA, 1964; pp. 4–39.
17. Clarke, J.I. *Morphometry from Maps: Essay in Geomorphology*; Elsevier Publishing Co.: New York, NY, USA, 1996; pp. 235–274.
18. Magesh, N.S.; Chandrasekar, N.; Soundranayagam, J.P. Morphometric evaluation of Papanasam and Manimuthar watersheds, parts of Western Ghats, Tirunelveli district, Tamil Nadu, India: A GIS approach. *Environ. Earth Sci.* **2011**, *64*, 373–381. [CrossRef]
19. Silva, M.T.; da Silva, V.D.; de Souza, E.P. Morphometric analysis of the basin low middle São Francisco river. *J. Hyperspectral Remote Sens.* **2014**, *4*, 168–174. [CrossRef]
20. Ehrenfried, L. Geographic information systems in mountain risk and disaster. *Appl. Geogr.* **2015**, *63*, 212–219.
21. Gravelius, H. *Flusskunde*; Goschen'sche Verlagshandlung: Berlin, Germany, 1914.
22. Horton, R.E. Drainage-basin characteristics. *Trans. Am. Geophys. Union* **1932**, *13*, 350–361. [CrossRef]
23. Smith, K.G. Standards for grading texture of erosional topography. *Am. J. Sci.* **1950**, *248*, 655–668. [CrossRef]
24. Schumm, S.A. Evolution of drainage systems and slopes in badlands at Perth Amboy, New Jersey. *Geol. Soc. Am. Bull.* **1956**, *67*, 597–646. [CrossRef]
25. Bull, W.B.; Mcfadden, I.M. Tectonic geomorphology north and south of the Garlock Fault, California. *Geomorphology* **1977**, *1*, 15–32. [CrossRef]

26. Verstappen, H.T. *Applied Geomorphology: Geomorphologicai Surveys for Environmental Development*; Elsevier: Amsterdam, The Netherlands, 1983.
27. Gregory, J.K.; Walling, E.D. *Drainage Basin Analysis*; The Bath Press: Armadale, VIC, Australia, 1985.
28. Maidment, D.R. *Handbook of Hydrology*; McGraw Hill: New York, NY, USA, 1992.
29. IDEAM—Institute of Hydrology, Meteorology and Environmental Studies. Geoportal—IDEAM. Available online: http://www.ideam.gov.co/geoporta (accessed on 27 January 2022).
30. IDEAM. *Caracterización Climática de la Evapotranspiración de Referencia (ETo) en Colombia: Distribución Espacio-Temporal, Variabilidad Interanual y Afectación por el Fenómeno el Niño-Oscilación Sur (ENOS)*; IDEAM: Bogota, Colombia, 2019.
31. Espinal, L.S. Zonas de Vida o Formaciones Vegetales de Colombia: Mapa Ecológico. In *Memoria Explicativa Sobre el Mapa Ecológico*; Instituto Geográfico Agustín Codazzi (IGAC): Bogota, Colombia, 1977; Volume 11, p. 13.
32. Instituto Geográfico Agustín Codazzi—IGAC. *Los Cañones Colombianos: Una Síntesis Geográfica*; Ciaf, O., Guzmán, I.D.G., Eds.; IGAC: Bogota, Colombia, 2007.
33. Rangel-Ch, J.O.; Cadena, A. Vegetation of the Chicamocha River Canyon (Santander, Colombia). *Caldasia* **2003**, *25*, 73–99.
34. Ward, D.E.; Goldsmith, R.; Jimeno, A.; Cruz, J.; Restrepo, H.; Gómez, E. *Geología de la Plancha 109 Rionegro*; Ingeominas: Bogota, Colombia, 1977.
35. Ward, D.E.; Goldsmith, R.; Cruz, J.; Jaramillo, L.; Vargas, R. *Geología de la Plancha 110 Pamplona*; Ingeominas: Bogota, Colombia, 1977.
36. Ward, D.E.; Goldsmith, R.; Jimeno, A.; Cruz, J.; Restrepo, H.; Gómez, E. *Geología de la Plancha 120 Bucaramanga*; Ingeominas: Bogota, Colombia, 1977.
37. Vargas, R.; Arias, A.; Jaramillo, L.; Tellez, N. *Geología de la Plancha 136 Málaga*; Ingeominas: Bogota, Colombia, 1984.
38. González, O.P. *Geología de la Plancha 135 San Gil*; Ingeominas: Bogota, Colombia, 1985.
39. Velandia, F.; Bermúdez, M. The transpressive southern termination of the Bucaramanga fault (Colombia): Insights from geological mapping, stress tensors, and fractal analysis. *J. Struct. Geol.* **2018**, *115*, 190–207. [CrossRef]
40. Siravo, G.; Fellin, M.G.; Faccena, C.; Maden, C. Transpression and build-up of the cordillera: The example of the Bucaramanga fault (eastern cordillera, Colombia). *J. Geol. Soc.* **2020**, *177*, 14–30. [CrossRef]
41. Naranjo, J.A.O.; Moreno, C.H.; Jaimes, E.M.T.; Santa, P.A.B. *Modelo Geodinámico del Macizo de Santander*; Ingeominas: Bogotá, Colombia, 2008.
42. IGAC. Agustín Codazzi Geographical Institute. Datos Abiertos. Available online: https://geoportal.igac.gov.co/contenido/datos-abiertos-cartografia-y-geografia (accessed on 1 November 2021).
43. ASF, A.P. Dataset: ASF DAAC 2015, ALOS PALSAR_Radiometric_Terrain_Corrected_Low_Res. Available online: https://asf.alaska.edu/data-sets/derived-data-sets/alos-palsar-rtc/alos-palsar-radiometric-terrain-correction/ (accessed on 1 November 2021).
44. Hack, J.T. *Studies of Longitudinal Stream Profiles in Virginia and Maryland*; US Government Printing Office: Washington, DC, USA, 1957; Volume 294, p. 95.
45. Strahler, A.N. Hypsometric (area-altitude) analysis of erosional topography. *Geol. Soc. Am. Bull.* **1952**, *63*, 1117–1142. [CrossRef]
46. Horton, R.E. Erosional Development of Streams and Their Drainage Basins; Hydrophysical Approach to Quantitative Morphology. *Geol. Soc. Am. Bull.* **1945**, *56*, 275–370. [CrossRef]
47. Diaz, M.A.R.; Bermúdez, F.L. Morfometría de Redes Fluviales: Revisión Crítica de los Parámetros Más Utilizados y Aplicación al alto Guadalquivir. *Pap. Geogr.* **1987**, *12*. Available online: https://revistas.um.es/geografia/article/view/42391 (accessed on 23 March 2022).
48. Keller, E.A.; Pinter, N. Active tectonics. In *Upper Saddle River*; Prentice Hall: Hoboken, NJ, USA, 1996; Volume 338.
49. Martonne, E. *Traité de Geographie Physique*; Armand Colin: Paris, France, 1940.
50. Fournier, F. *Climat et Erosion*; Presses Universitaires de France: Paris, France, 1960; p. 201.
51. Miller, V.C. *A Quantitative Geomorphic Study of Drainage Basin Characteristics in the Clinch Mountain Area, Varginia and Tennessee*; Project NR 389042; Technical Report 3; Columbia University, Department of Geology, ONR, Geography Branch: New York, NY, USA, 1953.
52. Patton, P.C.; Baker, V.R. Morphometry and floods in small drainage basins subject to diverse hydrogeomorphic controls. *Water Resour. Res.* **1976**, *12*, 941–952. [CrossRef]
53. Melton, M.A. The geomorphic and paleoclimatic significance of alluvial deposits in southern Arizona. *J. Geol.* **1965**, *73*, 1–38. [CrossRef]
54. Piacentini, D.; Troiani, F.; Servizi, T.; Nesci, O.; Veneri, F. SLiX: A GIS Toolbox to Support Along-Stream Knickzones Detection through the Computation and Mapping of the Stream Length-Gradient (SL) Index. *ISPRS Int. J. Geo Inf.* **2020**, *9*, 69. [CrossRef]
55. Perez, L. *Fundamentos del Ciclo Hidrológico*; Universidad Central de Venezuela: Caracas, Venezuela, 1979; Volume 38.
56. Chow, V.T.; Maidment, D.R.; Mays, L.W.; Saldarriaga, J.G. *Hidrología Aplicada*; No. 551.48 C4H5; McGraw-Hill: Bogota, Colombia, 1994.
57. Soil Conservation Service—SCS. *Urban Hydrology for Small Watersheds*; No. 55; Engineering Division, Soil Conservation Service, US Department of Agriculture: Washington, DC, USA, 1986.
58. California Highways and Public Works. *California Culvert Practice: Reprint of a Series of Technical Abstracts*, 2nd ed.; Department of Public Works, Division of Highways, State of California: Sacramento, CA, USA, 1955.
59. Kirpich, T.P. Time of Concentration of Small Agricultural Watersheds. *J. Civil. Eng.* **1940**, *10*, 362.
60. Témez, J.R. *Cálculo Hidrometeorológico de Caudales Máximos en Pequeñas Cuencas Naturales*; Dirección General de Carreteras-MOPU: Madrid, Spain, 1978.

61. Giandotti, M. *Previsione delle Piene e delle Magre dei corsi D'acqua*; Ministero dei LL. PP., Servizio Idrografico Italiano. Memorie e Studi Idrografici: Acireale, Italy, 1934; Volume 8.
62. Clark, C.O. Storage and the unit hydrograph. *Trans. Am. Soc. Civ. Eng.* **1945**, *110*, 1419–1446. [CrossRef]
63. Enderson, F.M.; Wooding, R.A. Overland flow and groundwater flow from a steady rain of finite duration. *J. Geophys. Res.* **1964**, *69*, 1531–1540. [CrossRef]
64. Salimi, E.T.; Nohegar, A.; Malekian, A.; Hoseini, M.; Holisaz, A. Estimating time of concentration in large watersheds. *Paddy Water Environ.* **2017**, *15*, 123–132. [CrossRef]
65. Hack, J.T. Stream-profile analysis and stream-gradient index. *J. Res. Us Geol. Surv.* **1973**, *1*, 421–429.
66. Hack, J.T. *Interpretation of Erosional Topography in Humid Temperate Regions*; Bobbs-Merrill: Washington, DC, USA, 1960.
67. Sala, M.; Gay, R. Algunos Datos Morfométricos de la Cuenca de Isábena. In *Notes de Geografía Física*; Department de Geografía, Universitat de Barcelona: Barcelona, Spain, 1981.
68. García-Delgado, H.; Villamizar-Escalante, N.; Matthias, B. Recent tectonic activity along the Bucaramanga Fault System (Chicamocha River Canyon, Eastern Cordillera of Colombia): A geomorphological approach. *Z. Geomorphol.* **2019**, *62*, 199–215. [CrossRef]
69. Velandia, F. Cinemática de las Fallas Mayores del Macizo de Santander—Énfasis en el Modelo Estructural y Temporalidad Al Sur de la Falla de Bucaramanga. Ph.D. Dissertation, Universidad Nacional de Colombia, Bogota, Colombia, 2017.
70. Amaya, S.; Zuluaga, C.; Bernet, M. *Different Levels of Exhumation Across the Bucaramanga Fault in the Cepitá Area of the Southwestern Santander Massif, Colombia: Implications for the Tectonic Evolution of the Northern Andes in Northwestern South America*; The Geology of Colombia: Bogotá, Colombia, 2020; Volume 3.
71. García-Delgado, H.; Villamizar-Escalante, N.; Bermúdez, M.A.; Bernet, M.; Velandia, F. Climate or tectonics? What controls the spatial-temporal variations in erosion rates across the Eastern Cordillera of Colombia? *Glob. Planet. Chang.* **2021**, *203*, 103541. [CrossRef]
72. Thornthwaite, C.W. An approach toward a rational classification of climate. *Geogr. Rev.* **1948**, *38*, 55–94. [CrossRef]
73. Albesiano, S.; Rangel-Ch, J.O. *Estructura de la Vegetación del Cañón del río Chicamocha, 500–1200 m; Santandercolombia: Una Herramienta Para la Conservación*; Caldasia: Santander, Colombia, 2006; pp. 307–325.
74. Mejía, I.S. *Geografía Económica de la Región Andina Oriental*; Banco de la República: Cartagena de Indias, Colombia, 2010.
75. Gómez-Heras, M.; Bernard, J.; Rafael, F. Surface temperature differences between minerals in crystalline. *Geomorphology* **2006**, *78*, 236–249. [CrossRef]
76. Richter, C. *Elementary Seismology*; W.H. Freeman: San Francisco, CA, USA, 1958.
77. Prieto, G.A.; Beroza, G.C.; Barrett, S.A.; López, G.A.; Florez, M. Earthquake nests as natural laboratories for the study of intermediate-depth earthquake mechanics. *Tectonophysics* **2012**, *570*, 42–56. [CrossRef]
78. Gutenberg, B.; Richter, C.F. Earthquake magnitude, intensity, energy, and acceleration: (Second paper). *Bull. Seismol. Soc. Am.* **1956**, *46*, 105–145. [CrossRef]
79. Kranz, R.L. Microcracks in rocks: A review. *Tectonophysics* **1993**, *100*, 449–480. [CrossRef]
80. Vanguardia. La Avalancha en Piedecuesta Arrasó Con Todo. Available online: https://www.vanguardia.com/area-metropolitana/bucaramanga/la-avalancha-arraso-con-todo-FD2063766 (accessed on 26 February 2020).

Disclaimer/Publisher's Note: The statements, opinions and data contained in all publications are solely those of the individual author(s) and contributor(s) and not of MDPI and/or the editor(s). MDPI and/or the editor(s) disclaim responsibility for any injury to people or property resulting from any ideas, methods, instructions or products referred to in the content.